Optimization of a plasma etching machine for failure analysis of semiconductors

by

Bingyan Xu

Student Name	Student Number
Bingyan Xu	5608066

Daily supervisor:	Prof.Dr. GuoQi Zhang
Thesis committee:	Prof.Dr. GuoQi Zhang
	Dr. K.M. Dowling
	Dr. Jiaqi Tang
Project Duration:	10, 2022 - 9, 2023
Faculty:	Faculty of EEMCS, Delft

This thesis is confidential and cannot be made public until December 31, 2025.

TU Delft

Optimization of a plasma etching machine for failure analysis of semiconductors

by

Bingyan Xu

to obtain the degree of Master of Science
at the Delft University of Technology,
to be defended publicly on Wednesday September 21, 2023 at 9:00 AM.

Student number:	5608066	
Project duration:	October 1, 2022 – September 21, 2023	
Thesis committee:	Prof. Dr. GuoQi Zhang,	TU Delft
	Dr. K.M. Dowling,	TU Delft
	Dr. Jiaqi Tang,	Jiaco Instruments

This thesis is confidential and cannot be made public until September 20, 2025.

TU Delft

Abstract

Microwave Induced Plasma (MIP) is an advanced decapsulation tool developed by Jiaco Instruments. Atmospheric pressure MIP decapsulation systems based only on O2 allow high etching selectivity of mold compounds with wires, bond pads, passivation layers, die etc. without introducing damage to the wires as well as artefacts. The MIP system has significant advantages over acid, CF4-containing conventional plasma decapsulation methods.

The goal of this thesis is to optimise the current MIP system. There are two directions: 1. The current MIP system often takes several hours to complete the decapsulation process of a sample, so it is highly necessary to improve the etching rate. 2. New CF4-based MIP systems are developed and in order to explore the application prospects of the new system, etching experiments between different materials (Si, SiO2, SiN) as well as selectivity between the materials are explored.

For the optimisation of the etching rate of the MIP system, the method of increasing the height of the Beenakker cavity with different thicknesses of copper rings is investigated. From the results of the cavity experiments at different heights, the plasma filament lengths remain essentially the same, and the etching rates for Si materials also remain the same. Therefore, increasing the cavity height to optimise the etching rate is not feasible. In this case, another experimental direction is proposed to experiment with a modified cavity to test whether a stable plasma can be consistently generated at high input power (>100W). From the experimental results, it was concluded that high power to optimise the performance of the MIP machine is a feasible direction.

To broaden the scope of MIP system applications, Jiaco Instruments has developed MIP machines based on CF4. The CF4/O2 MIP machine is highly needed to explore the etching selectivity between silicon (Si), silicon dioxide (SiO2) and silicon nitride (SiN) materials, which are commonly used in IC fabrication. From the experimental results, it is found that the introduction of CF4/O2 gas mixtures into the MIP system achieves acceptable results in terms of the etching selectivity between these different materials. In addition, etching experiments at different temperatures show that temperature also plays a critical role in influencing the etching performance of these materials.

Keywords: Microwave induced plasma(MIP), Afterglow plasma etching, Decapsulation, Beenakker cavity, Microwave power coupling, Etching recipe, Etching selectivity

Acknowledegments

Firstly, I would like to express my sincere appreciation to my tutor, Jiaqi, for his unwavering support and invaluable guidance over the past year. From the very beginning, during our initial meeting, Jiaqi introduced me to the MIP system. Subsequently, he patiently and carefully taught me to operate the MIP system manually. In addition, whenever I encountered difficulties in my research, Jiaqi generously offered advice, which was helpful in overcoming challenges and achieving meaningful results. His expertise and dedication have been a guiding light for me, for which I am deeply grateful.

I would also like to express my sincere gratitude to Prof. Beenakker. His guidance and insights helped me to find the path for my experiments, and his invaluable comments on this thesis contributed significantly to its depth and quality.

I would like to thank the team at Jiaco Instruments, including Lars, Lance, and all involved, for their support and assistance. Not only did they provide critical technical expertise, but their friendship over dinner made the research trip enjoyable and memorable. Thank you all so much for your support and friendliness, these experiences will remain a valuable part of my life.

I would like to express my heartfelt gratitude to my supervisor, Professor Kouchi, for his consistent support throughout my research. In addition, I express my gratitude to Professor Dowling for generously agreeing to be a member of my thesis committee and participate in the defence.

In addition, I would like to express my gratitude to all the professors and staff at ECTM and EKL. Their expertise and assistance, especially in training me to operate various laboratory equipment, has been instrumental in my research and overall academic development.

Last but not least, a sincere thank you to the family and friends who have been supporting me for the two-year study journey.

Contents

1

Introduction

1.1. Background

Microwave Induced Plasma (MIP) decapsulation system is a tool used in failure analysis, which is used for the decapsulation of packaged chips. The MIP system facilitates user access to a specific area of interest to determine the cause of the failure.

The beginnings of the MIP system can be traced back to Dr Jiaqi's PhD research between 2009 and 2013. Driven to innovate and address relevant challenges, he developed the MIP system during this period. His efforts resulted in a technology that uses microwave induced plasma to perform a controlled decapsulation process.

MIP has a number of advantages compared to the conventional decapsulation methods that are commonly used. Firstly, the acid decapsulation method damages copper wires, which are easily etched by acid as compared to gold wires. Secondly, conventional plasma etchers operating in a vacuum environment use CF4 & O2 as the etching gases, thus generating fluorine radicals that attack both Si3N4 and Si, which can cause unwanted over-etching damage to the chip. The MIP system avoids these drawbacks compared to these conventional decapsulation methods. At the same time, while developing the MIP system, Dr. Jiaqi charted a course to establish a commercial entity.[1]

This dual trajectory ultimately led to the formation of Jiaco Instruments - a business based on the ingenuity of the MIP system. As Jiaco Instruments grew and expanded its footprint, in keeping with the company's trajectory, Jiaco Instruments sought out students to be involved in research and development. [2]

Figure 1.1: MIP machine (Source: Jiaco Instruments)

The main goal of this thesis is to improve the performance of MIP machines. The core objective is to optimise the efficiency of the MIP system and to investigate in depth the potential paths that may be opened by the newly developed CF4-based MIP machines.

1.1.1. MIP Decapsulation System

The MIP system, which generates a stable plasma at atmospheric pressure, is an important tool for removing epoxy moulding compounds from integrated circuit (IC) packages. One of the most notable achievements of the MIP system is its ability to perform the decapsulation process without causing any undesired artefacts or damages to the wire bonding inside the IC package.

In addition, the MIP system has demonstrated the ability to achieve high levels of etching selectivity in atmospheric pressure oxygen MIP etching processes. This high etching selectivity is achieved at ratios above 1000:1 of the molding compound to various components such as wires, pads, passivation layers, and the die itself. The high selectivity is achieved by not using fluorine gas in the process. The MIP system avoids the introduction of fluorine gas that is expected in conventional plasma decapsulation, thus avoiding damage to critical passivation layers and molded components by excessive etching. This is critical as it maintains the structural integrity of the device during the decapsulation process, which is particularly beneficial for subsequent failure analysis work.[1]

One of the significant advantages of the MIP system is its excellent control level, which helps to locate the sample during the etching process accurately. This control mechanism ensures that specific areas of interest are precisely located and etched, thereby improving the accuracy and repeatability of results.[3]

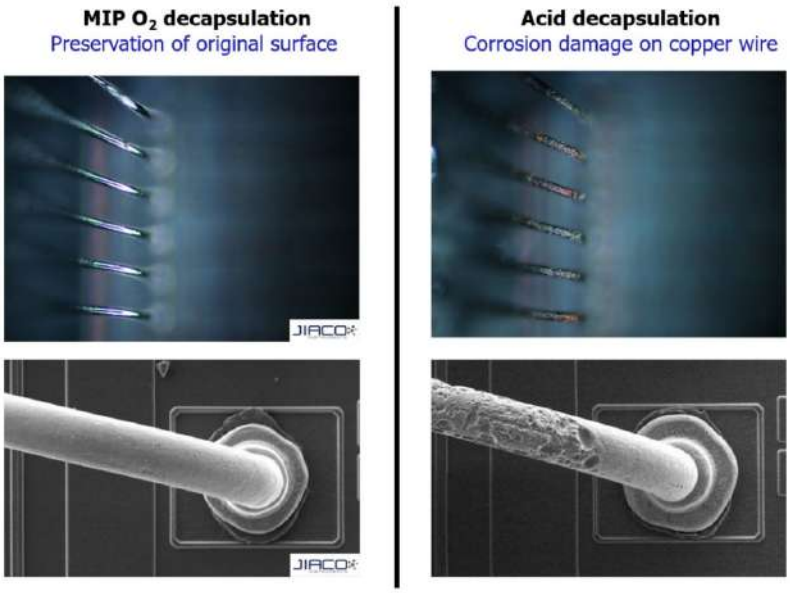

Figure 1.2: Comparison between MIP and Acid (Source: Jiaco Instruments)

Regarding reliability, the MIP system has excellent repeatability over multiple run times. This means that the system produces consistent results and is highly reliable in various applications.

1.2. Motivation and Objectives

1.2.1. Motivation

The aim of this thesis is to optimise existing MIP machines. However, to achieve a breakthrough in the market, the performance of existing MIP machines must be improved. This optimisation will be carried out along two distinct pathways:

1. Although current MIP equipment has successfully achieved the goal of etching packaging materials without damaging the integrity of the copper wire, there is still much improvement needed in the efficiency of the etching process. Currently, it may take several hours to etch a single sample before the entire etching process is complete. Therefore, the efficiency of the etching process on MIP equipment must be optimised. For this reason, Jiaco Instruments is looking to improve the etching rate by improving the structural design of the machine.

The main goal is simplifying and speeding up the etching process, significantly reducing the time required to complete the entire etching operation. It is expected that this optimisation work will completely change the efficiency of the MIP equipment, making the etching process faster and more efficient.

2. In recent years, Dr. Jiaqi Tang, Chief Technology Officer (CTO) of Jiaco Instruments, has led the way in developing a new device that uses CF4 gas as a core. This new equipment was developed from the original oxygen-based MIP system. The original oxygen-based MIP system could be used to selectively

etch epoxy in mold compounds. With the addition of CF4, new applications for MIP machines can be developed. CF4 gas, a common etchant used in plasma etching procedures, decomposes into fluorine atoms under the influence of high-energy particles. These fluorine atoms are effective in etching a variety of materials including silicon (Si), silicon nitride (Si3N4) and silicon oxide (SiO2).

1.2.2. Objectives

Based on the above motivation for this thesis, two different directions are planned to promote the field of plasma etching. These two directions include improving the Beenakker cavity and exploring CF4 machine etching selectivity. Specific objectives regarding these directions are shown below:

1. The primary goal of the first optimisation pathway is to increase the concentration of radicals in the plasma produced by the MIP machine. This purpose is expected to be achieved by increasing the height of the Beenakker cavity[4], which is an integral part of the MIP machine. This increase in radical concentration is expected to improve the etching process's efficiency significantly. Importantly, this optimisation will be carried out while maintaining a stable input power to ensure that the system's energy consumption remains constant.

2. The broader goal of this study is to perform detailed etching experiments using an innovative CF4-based MIP machine. Specifically, this study will focus on etching rates for three key materials: polysilicon, silicon nitride, and silicon oxide. In addition, this study attempts to reveal the complicated relationship between the etching selectivity of these three materials with respect to each other. By carefully conducting these empirical studies, this research aims to gain insight into these materials' unique etch properties and selectivity characteristics. The knowledge gained from these explorations will enrich the prospects of plasma etching technology and improve its development and application in different fields.

1.3. Thesis Outline

This thesis optimises the MIP machine in two ways: to make changes to the Beenakker cavity. The second one is the exploration of selectivity between different materials based on the latest CF4-based MIP machine. Fig.1.3 shows the structure of this paper.

- **Chapter 2:** The basic structure of the MIP system is presented in this chapter. Furthermore, the microwave characteristics of the Beenakker cavity are described in detail.
- **Chapter 3:** Optimisation of the Beenakker cavity is carried out in this chapter to validate the suspicion of improving the etching efficiency by increasing the cavity height and to verify the performance of a high cavity at high power.
- **Chapter 4:** This chapter uses a CF4-based MIP machine to explore the etching selectivity among three materials: silicon, silicon nitride, and silicon dioxide.
- **Chapter 5:** This chapter summarises this project and gives future work, especially in increasing the operating power.

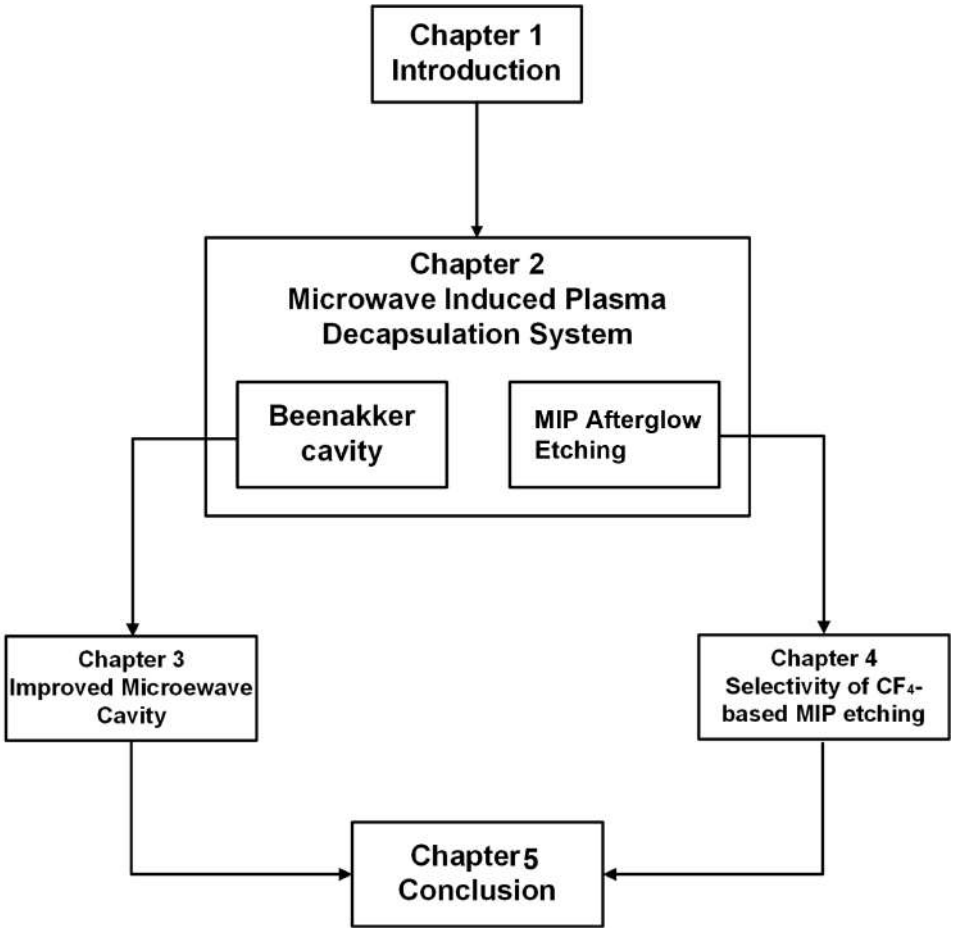

Figure 1.3: Thesis outline

2

Background Knowledge

This chapter provides an overview of the MIP system. Section 2.1 details the basic components of the system and their respective functions. Section 2.2 describes the microwave characteristics of the Beenakker cavity and introduces a modified version specifically tailored for MIP system applications. Section 2.3 provides an insight into the complex chemistry of the etching process of the MIP system.

2.1. Basics of MIP System

This section will briefly describe the MIP system. As shown in Fig.2.1, the MIP system consists of several key components, each of which plays a specific role in the process. The core of the system consists of a microwave generator, a Beenakker-type microwave resonant cavity, a gas discharge tube, a set of mass flow controllers (MFCs), a CCD camera, a programmable XYZ stage for precise positioning, and a computer for control.[3]

The microwave generator, model Sairem GMP20, can generate microwave signals from 0 to 200 W. In addition, the microwave signal frequency can be fine-tuned in the 2400 to 2500 MHz range to meet plasma generation requirements. In practice, however, the power of the microwave signal is limited to 60 W or less to ensure plasma stability.[5]

The role of the Mass Flow Controller (MFC) in the MIP system is to regulate the gas flow rate accurately. the number of MFCs is directly related to the number of gas species used in the etching process. These controllers allow for fine control of gas composition and flow rate, critical for uniform and repeatable etch results.

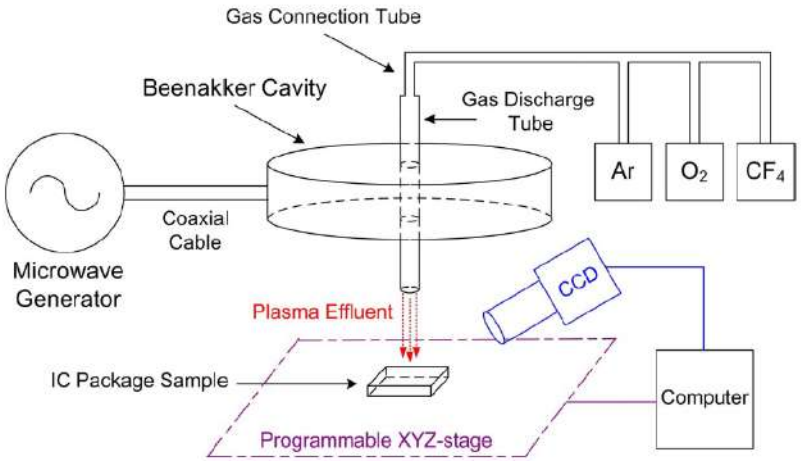

Figure 2.1: Schematic diagram of the MIP system

The CCD camera and programmable XYZ stage work in combination to enable precise positioning of the sample in the plasma for etching. This ensures that the target area in the sample is effectively targeted during the etching process.

However, one of the most critical components of the MIP system is the Beenakker-type microwave cavity. The resonator's design is critical as it significantly affects the stability and efficiency of the plasma generation process. The primary function of a resonant cavity is to generate and maintain plasma by exciting gas electrons with microwave energy. These electrons are accelerated in an electric field and collide with other gas atoms or molecules, creating more free electrons and leading to an avalanche effect of electrons. The avalanche of electrons leads to an extreme increase in the number of free electrons and the formation of a plasma.

The resonator cavities of the Beenakker-type cavity are carefully designed according to the plasma generation process. The cavity's design affects the generated plasma's stability and the concentration of ions and radicals in the plasma. The design parameters of the cavity are essential for obtaining a stable and efficient plasma, while the quality and accuracy of the plasma affect the etching process.

In addition, the cavity has an opening in the centre for inserting a gas discharge tube. The gas discharge tube is interconnected with the MFC to control gas injection at a predetermined flow rate. [3] The gas discharge tube is a critical component for introducing the type of gas required for plasma generation and etching.

In summary, the components of the MIP system work together to create a controlled and stable environment for the plasma generation and etching process. The Beenakker-type microwave cavity is the most important part of the MIP system, which directly affects the stability and efficiency of the plasma and is the foundation of the etching application of the MIP system. Integration of the various components ensures etching control that the MIP system achieves its goals in failure analysis and other applications.

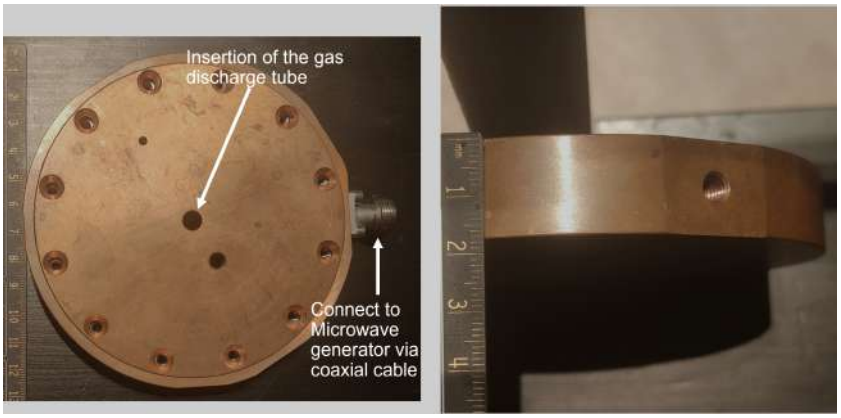

Figure 2.2: Top and front view of the Beenakker cavity

2.2. Microwave Induced Plasma Generation

The plasma generation can be controlled stably and efficiently based on the MIP system described above. In the gas discharge tube, argon, oxygen and CF4 are injected as etching gases and the gas flow is controlled by the MFC. At the same time, microwave power from a microwave generator is transmitted to the Beenakker cavity via a coaxial cable. A spark generator based on a Tesla coil ignites the plasma, causing an electric field in the cavity strong enough to ionise the gas molecules. Once the plasma is ignited, microwave energy is introduced into the system, exciting free electrons and ions and exposing them to a high-energy state. [3] These energetic free electrons and ions are the components of the plasma, and they can maintain the plasma by collisionally exciting other gas particles [6]. The magnitude and frequency of the microwave power can be adjusted to control the properties of the plasma.

2.2.1. Microwave Cavity

At the core of the MIP system is the Beenakker cavity, the critical component for plasma generation. Details of this key component are given below:

- **The original Beenakker cavity:** The Beenakker cavity is a breakthrough in MIP technology which Dr. C.I.M. Beenakker first developed in 1976. The design of this cavity, known as the TM010 resonant cavity, was a significant milestone as it allowed a low power plasma discharges to be realised in helium at atmospheric pressure, which is revolutionary in gas chromatography.[7, 8]

  As shown in Fig.2.2, a typical laboratory Beenakker resonant cavity has the shape of a pillbox with specific dimensions: an outer diameter of about 12 centimetres, a height of 2 centimetres and an inner diameter of 93.7mm. Importantly, it resonates at a frequency of 2.45 GHz. In the TM010 mode of operation, the electric field inside the cavity exhibits a unique pattern of minimum peripheral and maximum centre fields.

  When creating the MIP system, the Beenakker cavity was chosen because of its ability to provide

high power density and minimal stray fields[3].

- **Beenakker cavity in the MIP system:** During the development of the MIP system, there was one major challenge. Due to the burning of plasma inside the cavity, the electrical characteristics of the cavity changed. This resulted in a serious impedance mismatch in the original Beenakker cavity. To solve this problem, several improvements were introduced. A variable antenna was added and connected to the cavity via a coaxial connector. This antenna can be adjusted to achieve impedance matching and ensure efficient system operation.[3]

  All experiments discussed later in this thesis are based on the modified Beenakker cavity.

2.2.2. Plasma Stability

Ensuring plasma stability is important for a reliable and repeatable etching process. To maintain this stability in MIP system, several key methodologies are employed:

- **Precise Gas Flow Control:** To ensure plasma stability, gas flow rates and ratios must be precisely controlled. This level of control can be achieved with a MFC.
- **Microwave Power Control:** The microwave power supplied to the system plays a vital role in plasma stability. This control is achieved by managing the microwave generator through the PC operating system.
- **Antenna Glow:** In addition to these measures, the "point discharge" phenomenon must be resolved. When the input power exceeds a certain threshold, a phenomenon known as "breakdown" occurs in the resonant cavity. This phenomenon causes the plasma in the discharge tube to extinguish. Meanwhile, the tip of the variable antenna glows, displaying a form of metallic electrical discharge. This puzzling behaviour can be attributed to the breakdown event triggering enough ionisation to create a localised plasma near the tip of the antenna. The energy released manifests itself as visible light, illuminating the antenna tip. This may appear when using a Tesla coil-based spark generator for ignition. This phenomenon is often called "antenna glow" and occurs when the electric field strength around the antenna exceeds a specific threshold, as shown in Fig.2.3. To avoid this breakdown phenomenon, a multi-dimensional approach is proposed below: Firstly, the top of the variable antenna can be adjusted to a flat shape, thereby reducing the possibility of sharp metal points triggering a discharge. This design adjustment aims to minimise the circumstances under which a breakdown event can occur.

  Second, to mitigate "antenna glow" and improve stability, the spark generator responsible for ignition can be strategically placed at a location quite far from the plasma-generating cavity. This can dramatically reduce the possibility of tip discharges or antenna glows. This spatial separation minimises the strength of the electric field around the antenna during ignition, thus ensuring a more stable and controlled experimental environment.

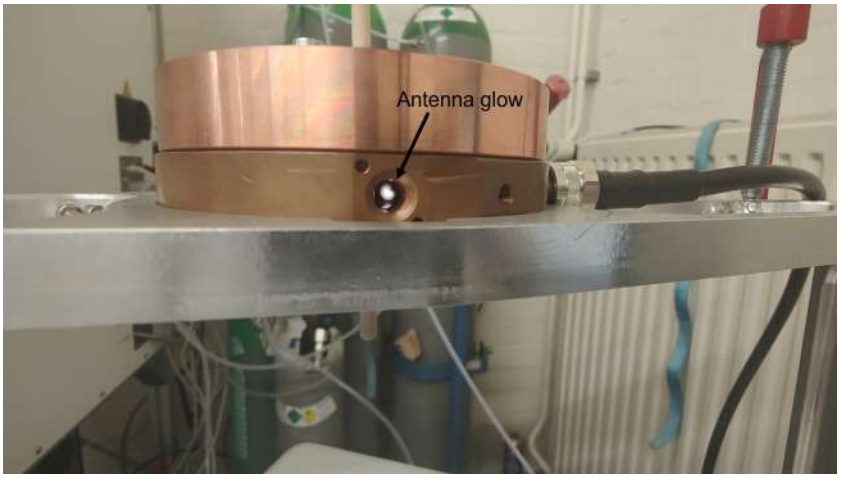

Figure 2.3: Antenna glow

2.3. Microwave Induced Plasma Afterglow Etching

2.3.1. Ar/CF4 Plasma Afterglow Etching

Once the plasma has been generated steady, the MIP machine places a Beenakker cavity with a gas discharge tube directly above the target sample. In this plasma, numerous chemically reactive species, especially ions and free radicals, are condensed and, due to the elevated energy levels, they exhibit incredibly high reactivity. Careful placement of the gas discharge tubes and the cavity is critical to ensure these highly reactive radicals are accurately introduced into the intended etching area.

In a plasma environment, chemically active species, including CF3- and F- ions,[9], however, in MIP afterglow etching, the F atoms dominate the plasma afterglow chemistry and the number of ions is almost absent, which means that no radiation damage occurs. The active fluorine atoms selectively interact with specific etching materials on the sample surface. This chemical interaction produces volatile compounds or by-products that quickly evaporate or are removed from the surface. This process eventually results in the etching of the desired pattern or structure on the samples.

By fine-tuning the composition of the gas mixture and optimising the process parameters (e.g. power, frequency, etc.), it is possible to control the achieved selectivity during the etching process tightly. Different materials are etched in the plasma at different rates so that specific ones can be removed highly selectively without altering others.

The unique properties of the MIP system make it particularly well-suited for the decapsulation of chips or electronic components.

2.3.2. Ar/CF4/O2 Plasma Afterglow Etching

Adding O2 to Ar/CF4 plasma significantly increases the etching rate. As the ratio of O2 to CF4 increases, the etch rate increases dramatically - peaking at about 30% O2[10]. However, as the O2 concentration increases, the etching rate decreases. This phenomenon can be attributed to complex

chemical interactions within the plasma.

Initially, when a small amount of O2 enters the CF4 plasma, the reaction between the CF3 radical and the O2 molecule leads to the formation of COF2 and an increase in the concentration of free fluorine (F) atoms [11, 12]. The increase in the concentration of free F atoms is an essential reason for the increase in the etching rate, as these particles play an important role in the etching process through positive interactions with the material surface.

However, the equilibrium effect becomes apparent with increasing O2 content. The concentration of CF4 molecules in the plasma decreases as the oxygen content increases. At the same time, the amount of chemically active species in the plasma, including CF3- and F- ions decreases, and the concentration of free F atoms also decreases. The reduction of the chemically active species affects the overall effect of the etching process, resulting in a lower etching rate.

In summary, adding O2 to Ar/CF4 plasma can accelerate the etching rate because of the increased generation of free F atoms. However, beyond a certain point, excess O2 leads to the depletion of the CF4 molecules and a decrease in the chemically active species, ultimately leading to a drop in the etching rate. These competing factors must be balanced to achieve optimal etching conditions.

2.4. Conclusion

This chapter introduces the MIP system and provides an insight into its core components and their roles, including the Beenakker cavity, the microwave generator, and the control module.

Most of the chapter is dedicated to revealing the microwave properties of the Beenakker cavity and explaining the effects of resonance properties and microwave distribution on plasma generation and etching. The chapter also shows the Beenakker cavity modified for use in the MIP system.

Finally, the chemical mechanisms involved in the etching process of the MIP system are illustrated. Understanding these reactions is essential to customising the system to achieve precise etching results for specific materials and applications.

In summary, this chapter provides a comprehensive overview of the components of the MIP system, focusing on the Beenakker cavity, microwave generator, and control module. The chapter also explores microwave characteristics, tuning procedures, and the chemical mechanisms at the core of the etching process.

3

Improved cavity

This chapter verifies the effect of the improved Beenakker cavity on the etching efficiency of the MIP system and the effect of power. In total, this chapter includes the following sections:

- **Section 3.1:** The increase in the height of the Beenakker cavity is assumed to improve the MIP etching efficiency. This section illustrates the theory that supports this speculation.
- **Section 3.2:** Impedance matching is required for the improved Beenakker cavity, and the methodology and results are shown.
- **Section 3.3:** Etching experiments were performed on the improved cavities and the results were compared with a different height of the cavities studied.
- **Section 3.4:** Experiments with high power input are performed on the improved cavity, and plasma with different cavity heights at various powers are compared.

3.1. Introduction

In downstream etching processes, increasing the cavity height of MIP system has been suggested to improve the overall etching efficiency[4]. The main objective is to manipulate the properties of the cavity to extend the residence time of the atoms involved in the etching process.

The cavity is where the plasma is generated and is the connection point between the microwave generator and the discharge tube. However, the plasma is mainly formed inside the discharge tube, which is crucial in the plasma generation process. The discharge tube is inserted into a cavity containing

a mixture of gases. A spark generator based on a Tesla coil ignites the plasma, and electromagnetic waves generated by a microwave generator are directed into a gas discharge tube in the centre hole of the cavity to maintain stable plasma generation. When the microwave energy is applied to the gas inside the discharge tube, it ionises and forms a plasma state. The plasma then flows from the discharge tube to the downstream of the cavity, which is the surface of the sample, where the etching occurs.

The key component of the MIP system is undoubtedly the Beenakker cavity. This specialised cavity plays an important role in keeping the microwave plasma at atmospheric pressure when operating at fairly low input power. The Beenakker cavity creates an environment that is conducive to keeping the plasma at atmospheric pressure, enabling a range of applications such as surface modification, thin film deposition and etching. Increasing the cavity height provides certain benefits. The higher the cavity height, the greater the expansion and flow volume of the plasma and the more uniform the distribution within the cavity.

Additionally, with the longer residence time of the atoms within the cavity, it can be assumed that the interaction time between the plasma and the surface of the material will also be extended, further increasing the possibility of a successful etching reaction, and the increased interaction time contributes to the etching efficiency. However, as the cavity height increases, the time for the reacting atoms to reach the surface of the sample also increases simultaneously, so whether increasing the cavity height will increase the etching rate of the MIP cannot be predicted and needs to be tested in experiments.

In summary, although the plasma is primarily generated within the discharge tube, there may still be benefits to increasing the height of the cavity in the MIP machine. It has been presumed that this would result in a more uniform distribution of the plasma within the cavity, thereby promoting a more consistent interaction with the material being etched. The extended residence time of the atoms in the cavity also promotes enhanced interaction between the plasma and the surface of the material, thereby improving the overall etching efficiency.

Figure 3.1: Copper rings of different heights (5mm, 10mm, 20mm)

Increasing the height of the Beenakker cavity is to use a copper ring made of the same material as the cavity, which is available in 5mm, 10mm, and 20mm sizes as shown in the Fig.3.1. The internal height of the original Beenakker cavity is 10mm, which means that the height of the cavity can be 1.5x, 2x, 2.5x, or 3x as high as the original one by adding copper rings.

However, as the height of the original cavity increased, problems occurred, a significant impedance mismatch began to appear within the MIP system. This change causes the MIP system to produce a large percentage of high reflected power, in excess of 50%. As shown in Fig.3.2, the original cavity could achieve 0% reflected power. However, with the use of copper rings to increase the cavity height, the reflected power can be up to 50% or more, as shown in Fig.3.3. Unfortunately, this can have a number of undesirable effects, in particular plasma instability and a significant reduction in the overall efficiency of the system. The effects of this impedance mismatch are quite severe. High reflected power greatly increases the instability of the plasma.[13] This instability destroys the accuracy and uniformity of the plasma behaviour and prevents the etching process from taking place in an ideal environment. In addition, the significant power loss due to reflections directly affects system efficiency, resulting in inefficient input power utilisation.

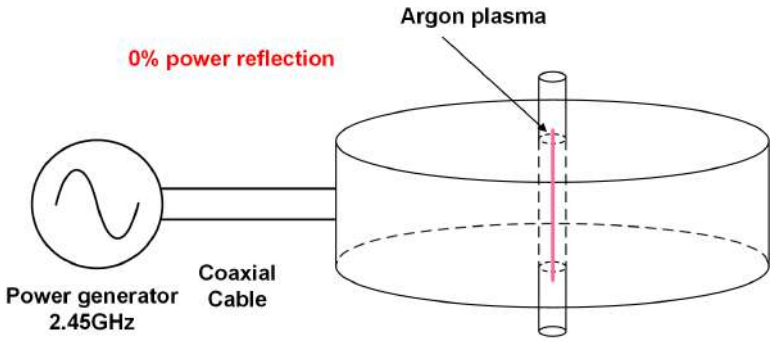

Figure 3.2: Schematic diagram of the original MIP system (low reflected power)

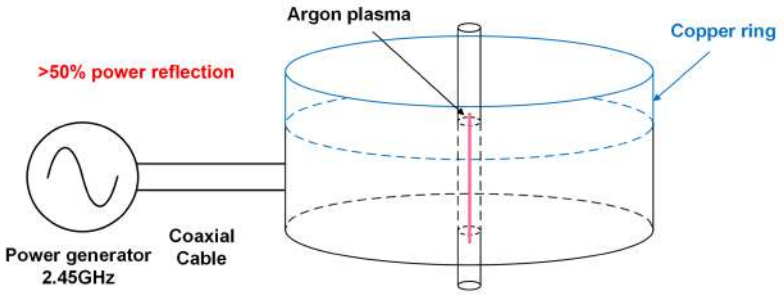

Figure 3.3: Schematic diagram of MIP system after adding copper ring (high reflected power)

This makes it necessary to resolve the impedance mismatch problem. Correcting this difference allows for an accurate evaluation of the expected improvement in cavity etch results. Corrective action would certainly include modifications to the Beenakker cavity to realign the electromagnetic

characteristics of the cavity with the modified cavity configuration, thereby reducing the impedance mismatch problem. In summary, although the theory was promising, the decision to increase the height of the original cavity created a significant impedance mismatch within the MIP system. This mismatch had multiple negative effects - plasma instability, reduced system efficiency, and inconsistent etching results. The impedance mismatch must be resolved because only when it is resolved can the etching potential of the improved cavity be accurately estimated.

3.2. Solve Impedance Mismatch

In current MIP machines, the tuning of the Beenakker cavity is critical. It has a variable antenna that attaches a coaxial connector to the cavity. In the original design, the length and position of the variable antenna were carefully tuned to support the stable generation of argon, CF4, and oxygen plasma at 60W input power.[3]

However, changing the cavity height through the copper ring shifts the internal electromagnetic field pattern. This shift increases the reflection rate to over 50%, compared to the previous nominal reflection of 0%, resulting in plasma instability. The need for retuning became apparent, and experimental results confirmed that recalibrating the length and positioning of the antenna to achieve a reflection of 0% of the restored the required plasma stability. In summary, the role of the Beenakker cavity in the MIP machine is critical to stabilising plasma generation. Changing the height of the cavity with a copper ring disrupts the power reflection and requires retuning. Adjusting the length and position of the original antenna can achieve the desired results.

3.2.1. Power Reflection Analysis

The impedance mismatch in the higher cavities must be resolved before performing the actual etching experiment. High reflected power causes a number of problems. High reflected power means that a part of the microwave energy is reflected back to the source and not transferred efficiently to the plasma.

- **1.** The first and foremost problem is that the plasma cannot be generated stable. A large amount of microwave energy being reflected back may result in insufficient energy input, leading to plasma extinction or instability.
- **2.** Secondly, the high reflected power may lead to overheating of the equipment, especially the Beenakker cavity and the variable antenna within it, which may be damaged.
- **3.** Finally, high reflected power may cause damage to the magnetrons in the microwave generators in the MIP system.

The experimental equipment used to complete the impedance matching was a manual test setup, as Fig.3.4 below shown. The test setup is a simple MIP system consisting of a microwave power generator, a Beenakker cavity with a copper ring, a gas cylinder to provide argon gas, a Mass Flow Controller, and

a spark generator to excite the plasma. The reason for using a manual test setup is that the cavity allows for easy adjustment of the internal variable antenna anytime, which is a critical component in the tuning process, and whose spatial position and length can lead to changes in the electric and magnetic field distributions, which in turn affects the impedance. The overall goal is to achieve impedance matching by varying the input impedance, thus enabling a transition from an off-centre configuration to a fully resistive centre (50 ohms).

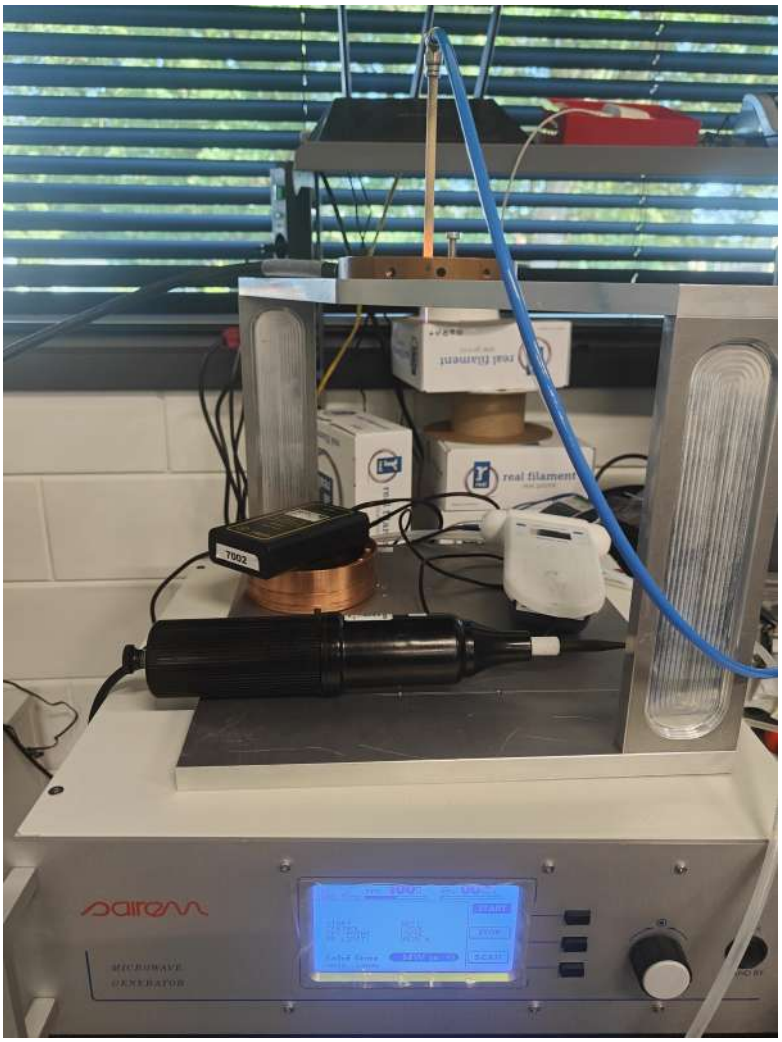

Figure 3.4: Manual test setup

Fig.3.5 shows the cavity with perfect impedance matching, and you can see an argon plasma filament in the gas discharge tube. The filament length of the plasma is an illuminating criterion that describes the microwave power absorbed by the plasma.[14] Tab.3.1 below demonstrates the interaction between reflected power and argon filament length with the addition of copper rings of different heights to the primary cavity after impedance matching. The efficacy of the variable antenna remains even when the cavity is raised. This is demonstrated by the precise operation of the variable antenna characteristics, where the enlarged cavity has a reflected power of 0

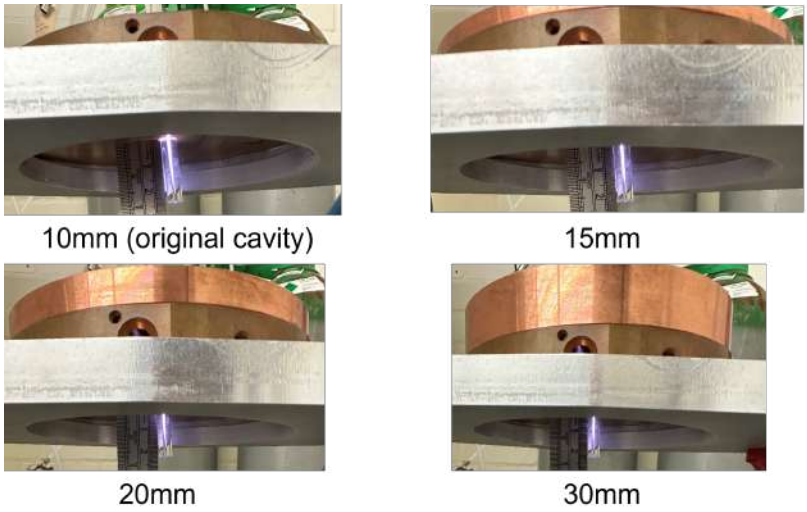

Figure 3.5: Higher cavity with stable Ar plasma

Meanwhile, filament lengths of cavities of different heights are shown side-by-side at lower reflectivity conditions (below 0.1), and they are nearly equal at an equivalent 20W input power level. It is worth noting that these experimental results call into question the initial conjecture regarding the height of the cavities. However, etching experiments were necessary to confirm the validity of the earlier assumption. There are two reasons for this: Firstly, although filament length positively correlates with the absorbed plasma power, the actual etching process is intricate. Sample temperature, plasma reactant density, and microwave power contribute to the etching process. Secondly, the positive correlation between filament length and absorbed plasma power is only one aspect. Direct measurements of the atomic energy density of the etched plasma remain elusive, and etching experiments are needed to test the hypothesis. It is worth noting that although the filament lengths of the plasma produced by cavities of different heights are almost equal during the measurement process, there is still the possibility of measurement discrepancies, which need to be empirically verified by etching experiments.

3.2.2. Effects of Different Gas Recipes

As shown in Fig.3.4, it is clear that impedance matching of the higher cavity was previously accomplished through a manual test setup.[3] It is worth noting that the unit lacks an exhaust gas treatment unit. As discussed in 2, the etching gas currently used within the MIP machine consists primarily of CF4 and O2. In CF4 and O2 plasma etching, toxic and corrosive by-products are released. For example, during etching with CF4 plasma, fluorine atoms may react with hydrogen or water molecules in the air to produce hydrofluoric acid (HF). In addition, by-products of O2 plasma include compounds such as ozone and nitrogen oxides. Considering these factors, it is essential to incorporate an exhaust gas treatment process into the actual etching process.

It is important to note that the manual test setup used in the previous experiments was initially designed for an argon plasma environment. However, the introduction of etchant gas triggers a

Table 3.1: Reflected power and filament length after adding copper ring

Cavity height (mm)	Filament extension below cavity (mm)	Power input (W)	Power reflected (W)	Ar (sccm)	Frequency(MHz)
10 (original cavity)	17	30	10	1400	2400
15	15	21	1	1400	2400
20	14	21	1	1400	2400
30	14	23	3	1400	2400

phenomenon known as plasma detuning. [3] This effect arises due to the high electronegativity of O2 and CF4, which tend to trap free electrons and promote the formation of oxygen ions. As a result, this electron trapping mechanism decreases electron concentration, affecting the delicate balance of the ionisation process. As a result, the addition of etchant gases disrupts the resonant properties of the previously well-matched Beenakker cavity. With each increase in the amount of etchant gas introduced, a clear trend emerges: the visual appearance of the plasma darkens, and the reflected power level increases.

In light of these findings, it became critical to thoroughly investigate the effect of etchant gas introduction on cavity resonance matching. An essential requirement imposed by this study was that the power reflectivity had to be carefully controlled to ensure that it remained at an efficient level (<0.1) after adding the etchant gas. Such stringent conditions are necessary to safeguard the stability and performance of the plasma system. Fig.3.6 below shows that a stable Ar/O2 plasma can be generated by adding copper rings of different heights to the cavity.

Next, the tuned cavity was installed in the MIP machine, and dummy tests were performed with CF4 plasma, O2 plasma and CF4+O2 mixed plasma. After several careful adjustments of the variable antenna and frequency, the different cavity heights were each able to produce stable plasma at efficient reflectivity conditions. This process succeeded in reducing the reflectivity problem during plasma formation. Notably, in this case, the argon plasma has a relatively high reflectivity, whereas the CF4 plasma, the O2 plasma, and the mixed CF4+O2 plasma have a low reflectivity in comparison. With these results obtained in the experiment, we can confidently move on to the next stage of the etching investigation.

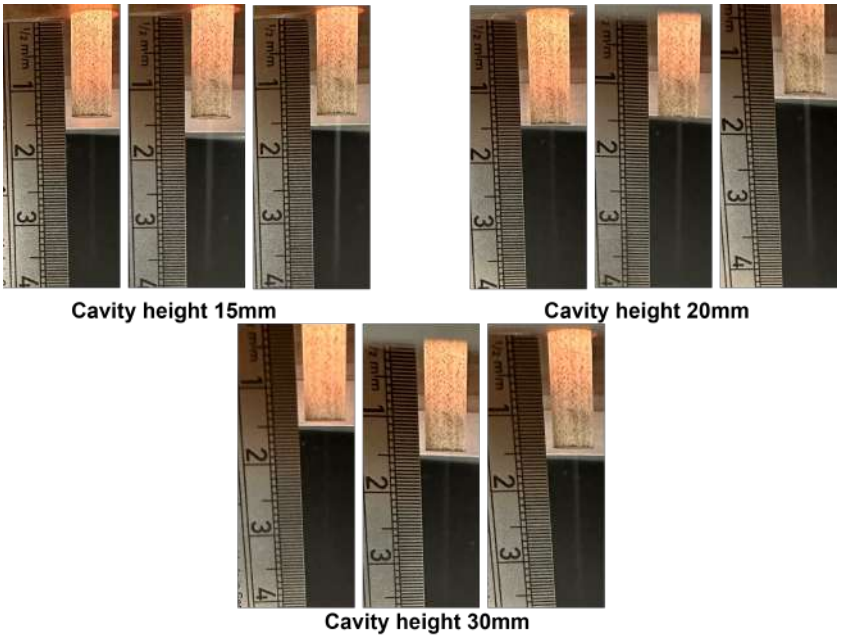

Figure 3.6: Higher cavity with stable Ar/O2 plasma (30W, 1400sccm Ar, 2400MHz)

3.3. Improved Cavity Etching Results

After the cavity modification, the etching experiment entered a new phase. An impedance-matched Beenakker cavity replaced the original cavity. It is worth noting that the screws surrounding the outer layer of the cavity were intentionally left out to allow the cavity to be impedance matched again. This design feature allows for easy adjustment of the variable antenna for optimal impedance matching.

All other parameters related to the etching process remain unchanged. This includes factors such as the etch material, the particular etch recipe employed, the input power level, and the duration of the etching process. However, an adjustable aspect is introduced by manipulating the microwave frequency centred at approximately 2450MHz. This dynamic frequency adjustment is used to fine-tune the microwave plasma, ensuring the reflected power level remains relatively low.

Polycrystalline silicon wafers were selected as the designated etching material for these experiments. This choice meets the requirements for producing microelectronic devices, building integrated circuits and fabricating other semiconductor components. [15] The specific etching material was not of primary importance in verifying the high-cavity effect of the MIP machine. Therefore, off-the-shelf bare silicon wafers were used in subsequent etching experiments.

Under ambient conditions and over time, a layer of silicon oxide (SiO2) naturally forms on the surface of silicon. This layer, known as the "natural oxide layer" or "oxide film", consists mainly of silicon dioxide (SiO2) and is the result of the interaction of the silicon material with atmospheric oxygen. The natural oxide layer can reach a thickness of about 2 to 3 nanometres [16] after exposure to air for a few hours to a few days under typical room temperature conditions. However, given its relatively small thickness, this layer is irrelevant and negligible for etching experiments.

An Ar/CF4/O2 gas mixture was chosen for the etching process. Argon (Ar) was the plasma carrier gas at a constant flow rate of 1400 standard cubic centimetres per minute (sccm). Oxygen (O2) and carbon tetrafluoride (CF4) were used as the plasma etching gases, with a flow rate of 10 sccm/min for CF4 and 5 sccm/min for oxygen. This particular combination was chosen based on a study by Jiaqi[10], which showed that the highest etch rates for silicones were achieved when the CF4 content of the O2/CF4 etching gas mixture was between 65% and 85%. In this experiment, the CF4 content was set to 75%, resulting in a relatively high etch rate. This setting is favourable to produce a more pronounced etching depth in a shorter etching time.

The power of the microwave can also affect the properties of the plasma; increasing the microwave power can increase the degree of ionisation and temperature of the plasma, thus changing its properties. The etching experiments were done in two groups based on the same high cavity with input power of 30W and 50W to investigate the effect of power. The etching time was kept at constant in each set of experiments.

Table 3.2: Etching experiments on silicon with different heights of cavity

Cavity height (mm)	Input Power (W)	Etching Time (min)	Frequency (MHz) (W)	Gas Flow	Etch Rate (um/min)
10 (original cavity)	30	5	2450	1400Ar 10CF4 5O2	4.44
15 (original cavity)	30	5	2465	1400Ar 10CF4 5O2	3.5
20 (original cavity)	30	5	2450	1400Ar 10CF4 5O2	4.76
25 (original cavity)	30	5	2430	1400Ar 10CF4 5O2	4.44
25 (original cavity)	50	5	2445	1400Ar 10CF4 5O2	11.92
25 (original cavity)	50	5	2450	1400Ar 10CF4 5O2	11.65
25 (original cavity)	50	5	2455	1400Ar 10CF4 5O2	12.00
25 (original cavity)	50	5	2430	1400Ar 10CF4 5O2	11.43

Under the tightly controlled conditions elucidated earlier, the experimental results yielded the subsequent observations. The results of the etching experiments are shown in Fig.3.2 and the etching profile is displayed in Fig.3.7. The etching profile shown closely resembles the conical structure. The distinguishing feature of the etching process is the height difference in depth between the surface of the silicon wafer and the central vertex of the etch profile, also known as the etch depth, which is an important metric to quantify the extent of material removal during the etching process. At the same time, use the volume formula of the cone to calculate the effective etching volume.

$$V_{cone} = \frac{1}{3} * Etchingarea * Etchingdepth \tag{3.1}$$

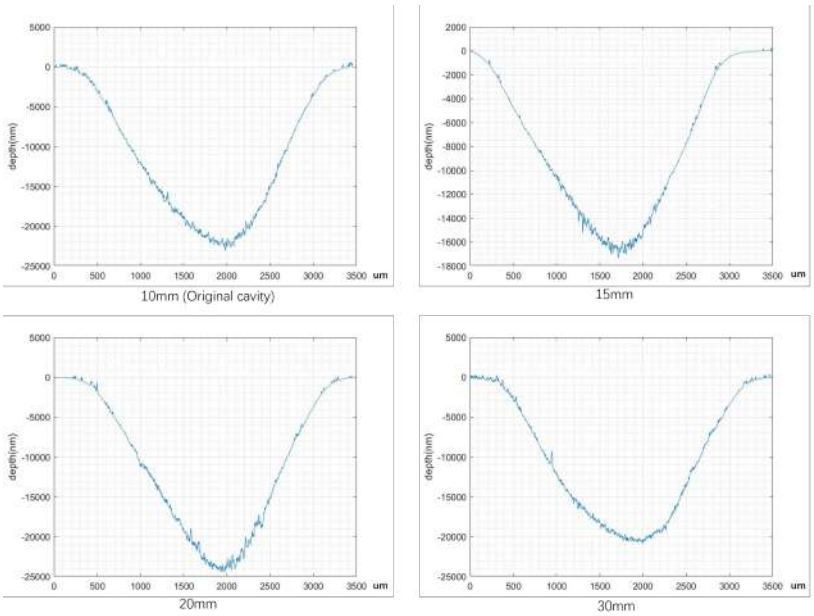

Figure 3.7: Profiles of Si etching with different heights of cavities (10sccm CF4, 5sccm O2)

A careful reading of Tab.3.2 in the combined data set reveals a critical revelation: increasing the cavity height has a negligible effect on the etching rate. This feature is evident at both low and high input power conditions, highlighting the etching process's robustness to cavity height changes. Analysis of the data demonstrates that changes in cavity height do not result in a significant difference in etch rate regardless of the input power used.

In the preceding manual test setup, from Tab.3.1 in the data, a consistent pattern emerges: the length of the plasma filaments produced by varying cavity heights is very uniform. This apparent uniformity emphasises an important point - the magnitude of the energy delivered to the plasma via microwave excitation remains essentially constant. Consequently, the degree of ionisation within the plasma, the concentration of reactive ions or radicals (e.g. F-, CF3-, O-) produced by the etching gas, and the resulting etch rate also show negligible deviations.

This is further confirmed by the observation in Fig.3.7, which reveals the impressive consistency of the etch profiles at different cavity heights. In essence, the etch profiles produced by different cavity heights are similar.

3.4. The Power Range of Improved Cavity

The results in Section 3.3 show that the improved cavity structure does not inherently improve the etching efficiency. However, a deeper look into the impedance matching process reveals an intriguing aspect. Beenakker cavities with different heights require a careful tuning process to keep the reflected power below the 0.1 critical value while maintaining a consistent position of the tuner unit.

To explain this interesting phenomenon, it is essential to recognise the critical role of the dimensions of the resonant cavity in facilitating the efficient transfer of microwave energy into the plasma. Specifically, the resonant cavity's height can potentially affect the shape and distribution of resonant modes. Different resonant ways produce unique electric field patterns within the cavity, which are closely related to the geometry and dimensions of the resonator.[6] Adjusting the height of the cavity can potentially result in the excitation of different resonant modes, each with its own specific electric field distribution. Therefore, any change in the height of the resonant cavity has the potential to alter the alignment between the input microwave energy and the resonant modes.

Indeed, to achieve optimum energy transfer, careful consideration must be given to the frequency and power adjustments of the input microwave signal. These adjustments ensure harmonious resonance with the dominant resonant mode and maximise energy transfer efficiency.

In contrast to the assumption of increased etch rate, another assumption is the potential for increased input power. The underlying assumptions suggest that higher cavities have the potential to accommodate higher input power levels that are consistent with the characteristics of the current resonant mode. It is worth noting that an increase in input power is directly related to the rise in the etch rate of the MIP machine. The basic principle behind this effect is that higher input power intensifies the ionisation and excitation processes between gas atoms, ultimately increasing the concentration of etched particles in the plasma medium.[17]

Therefore, the experiments in this section aim to critically assess whether a highly increased cavity can maintain plasma stability in the presence of elevated input power levels. It should be emphasised that existing Beenakker cavity configurations successfully enabled stable generation of argon, CF4 and oxygen plasma at 60W input power. Therefore, the primary goal of these experiments was to successfully tune the cavity to generate stable plasma at the higher input power threshold of 100 W. The primary purpose of these experiments was to successfully adjust the cavity to create stable plasma at the higher input power threshold of 100 W.

To facilitate these experiments, we again used the experimental setup used in Section 3.2, i.e. the manual test setup. This practical choice stems from the inherent limitations of current MIP machines, which prevent easy adjustment of power levels. In contrast, the manual test setup allows direct control of the input power via the generator knob, allowing for better control of the experimental conditions. Although the gases used in the experiment were still limited to argon, which is not fully compatible with natural etching environments, this precaution was implemented to ensure a controlled and safe experimental environment.

Once the experimental equipment was configured, the power increase experiment began. Initially, the input power needed to be set at a conservative 20W level, resulting in plasma ignition and a subsequent decrease in power reflectivity. Subsequently, as the input power to the microwave generator was progressively increased, there was an observable gradual increase in reflectivity, creating an intriguing pattern of behaviour.

Table 3.3: Power reflection of different input power with different heights of cavity

10mm (original cavity)				**15mm**			
Input power(W)	**Frequency (MHz)**	**Reflected power(W)**	**Ar filament length(cm)**	**Input power(W)**	**Frequency (MHz)**	**Reflected power(W)**	**Ar filament length(cm)**
20	2435	2	2.9	20	2430	1	3
30	2435	1	4.1	30	2430	1	4
40	2435	1	5.4	40	2430	1	4.8
50	2435	2	6.4	50	2420	1	5.5
60	2435	2	7.2	60	2420	1	6.3
70	2435	3	7.7	70	2415	1	6.2
80	2435	3	8.2	80	2415	1	6.6
90	2435	3	8.5	90	2415	1	6.9
100	2435	3	9.7	100	2415	1	7.4
110	2435	3	8.9	110	2410	1	7.6
120	2435	3	8.9	120	2410	1	7.6
130	2435	4	8.9	130	\	No Plasma	\
140	2440	4	8.9	140	\	No Plasma	\
150	2440	4	8.9	150	\	No Plasma	\
160	2440	8	8.9	160	\	No Plasma	\
20mm				**30mm**			
Input power(W)	**Frequency (MHz)**	**Reflected power(W)**	**Ar filament length(cm)**	**Input power(W)**	**Frequency (MHz)**	**Reflected power(W)**	**Ar filament length(cm)**
20	2435	4	2.8	20	2430	0	3.2
30	2400	3	3.5	30	2430	0	3.9
40	2400	2	4.5	40	2420	0	4.4
50	2400	2	5	50	2420	1	4.8
60	2400	2	5.4	60	2420	2	4.9
70	2400	2	5.9	70	2415	2	4.9
80	2400	2	6.3	80	2415	3	5.3
90	2400	2	6.5	90	\	No Plasma	\
100	2400	3	6.8	100	\	No Plasma	\
110	2400	3-4	7	110	\	No Plasma	\
120	2400	4	7.2	120	\	No Plasma	\
130	2400	5	7.2	130	\	No Plasma	\
140	\	No Plasma	\	140	\	No Plasma	\
150	\	No Plasma	\	150	\	No Plasma	\
160	\	No Plasma	\	160	\	No Plasma	\

By analysing the data in Tab. 3.3, an interesting trend can be observed in the behaviour of different

cavity heights under other input power conditions. A cavity with an initial height of 10 mm can remain stable even when the input power is increased. In contrast, a cavity with a height of 15 mm can remain stable when the input power rises to 130W. This noteworthy result indicates that the cavity with increased height effectively maintains plasma stability even at higher input power levels than the original configuration. These findings imply that the input power capability of the MIP system could potentially be increased, a step that could result in a considerable percentage increase - which would undoubtedly significantly improve the overall etch efficiency.

One point of interest is the performance of the 25 mm cavity, which did not perform as expected compared to the 15 mm high cavity. A plausible explanation for this difference is that the variable antenna was not optimally tuned for impedance matching in the case of the 25 mm cavity.

However, when considering the effect of high input power levels, the Antenna glow phenomenon, previously mentioned in section 2.2.2, occurs. That is when a spark generator based on a Tesla coil is used for ignition, and a phenomenon known as "breakdown" appears in the resonant cavity. So that the strength of the electric field around the antenna exceeds a specific threshold, the tip of the antenna glows.

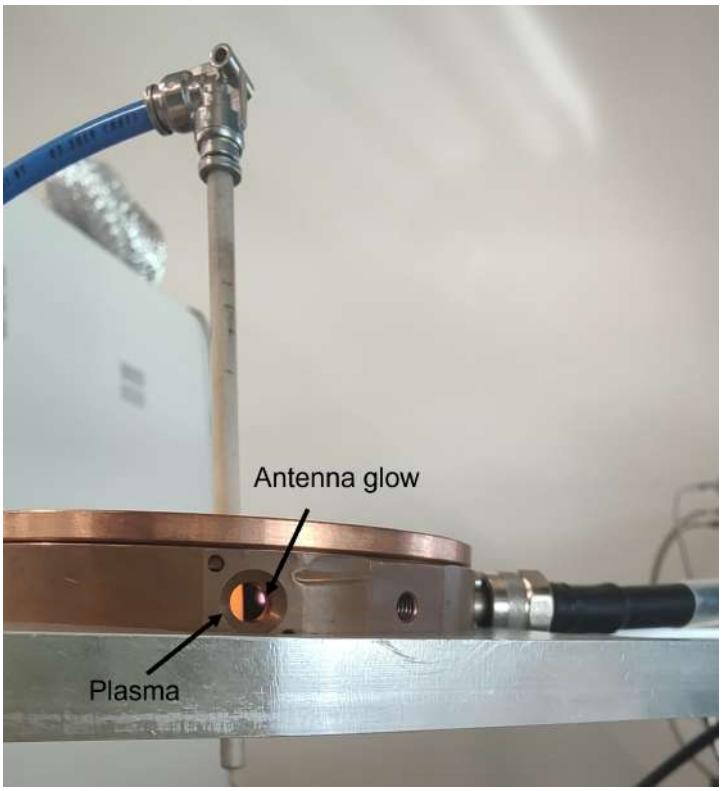

Figure 3.8: Antenna glow at high input power

At the time of the current experiment, however, Antenna glow occurs at extremely high input power. At this point, the plasma does not go out, as shown in Fig.3.8. Since the Antenna glow completely changes the microwave characteristics in the resonant cavity, the reflected power increases instantaneously, and the input power is adjusted to a low input power for safety reasons. At the lower

input power, the plasma and the Antenna glow phenomenon also exist.

This phenomenon undoubtedly affects the etching, but unlike the breakdown that occurs during ignition, no solution to this problem has been found so far.

3.5. Conclusion

Chapter 3 verifies the effect of the improved Beenakker cavity on the etching efficiency of the MIP system and the impact of power. The improved conjecture is that increasing the height of the Beenakker cavity enhances the efficiency of the MIP system, and impedance matching is accomplished.

However, upon rigorous experimentation and analysis of the results, it becomes evident that the modified Beenakker cavity does not significantly enhance the system's etching efficiency as initially anticipated. In response to these findings, a subsequent round of testing is conducted, employing an improved cavity design. The objective is to determine whether a stable plasma could be consistently generated at higher input power levels.

The outcomes of these follow-up experiments provide crucial insights. They indicate that higher power levels represent the optimal direction for fine-tuning and optimizing the MIP machine's performance.

4

Selectivity

4.1. Introduction

This chapter focuses on an in-depth look at the etching selectivity of various materials, particularly polysilicon, and two different silicon compounds: silicon nitride and silicon dioxide. The need for this research stems from the current demand for etching of inorganic materials. Polysilicon plays a pivotal role in the substrate of the semiconductor manufacturing process and is the basis for the careful fabrication of all semiconductor devices. Silicon dioxide is often used as a barrier layer to isolate different electronic components on a chip.[18] Silicon nitride, on the other hand, plays a significant role as a passivation layer for passivation and protection.[19] Our primary goal is to reveal the selectivity between these three different materials. This exploration is substantial because it has practical implications for engineering applications, as etching selectivity is a decisive factor in the final result.

In addition, it is worth noting how to determine the etching rate for each material. This parameter is significant because it will play a key role in future work. The etching rate indicates the rate at which material erosion occurs during the etching process and is a critical factor in material manipulation. Understanding the etching rate of different materials, including polysilicon, silicon nitride, and silicon dioxide, can help improve the etching process parameters and achieve accurate results.

4.2. Literature Study

We reviewed the available literature for additional insights to obtain the desired etching selectivity in these three materials.

Loewenstein et al.[20] found that the addition of O2 to fluorine-containing gases in remote microwave plasma gases significantly affected the etch rate and the etching selectivity for SiO2 and Si. For F2/He etchant mixtures, adding O2 decreased the etching ratio from 40:1 in the absence of O2 to 1:1. For CF4, the ratio was reversed from an initial 10:1 to less than 1:3. The mechanism is to affect the etching behaviour by altering the selective deposition of fluorocarbon polymers on Si.

Blain et al.[21] propose that achieving an efficient etch rate for silicon nitride (Si3N4) through chemical downstream etching necessitates the introduction of nitrogen into the discharge. This adjustment results in a substantial six-fold augmentation in the etch rate of Si3N4, coupled with an 8% reduction in the etch rate of silicon dioxide (SiO2), significantly enhancing the selectivity between these two materials. The observed and experimental upsurge in the Si3N4 etch rate is attributed to NO formation within the discharge. It is postulated that this phenomenon results from the direct interaction between NO and the Si3N4 surface.

Kastenmeier et al.[22] discovered that achieving selective etching of Si3N4 on Si and SiO2 could be accomplished by employing substantial quantities of O2 and N2 gases in conjunction with comparatively smaller quantities of CF4 and NF3 as sources of fluorine. The etching rate of Si3N4 was constrained by the influx of F atoms to the surface, and the elevation in the Si3N4 etching rate due to the heightened NO concentration in the chamber was insufficient to attain a substantial etch rate ratio. Consequently, they postulated that the principal mechanism for achieving a high Si3N4 etch rate ratio involved the formation of an inhibitory etching reaction layer atop the Si surface.

Loewenstein et al.[23] significantly improved the etch rate ratios of Si3N4:Si and Si3N4:SiO2 by adding an extractable hydrogen source (e.g., H2 or CH4) to the gas. Hydrogen depletes atomic fluorine and promotes preferential deposition of a fluorocarbon layer on Si and SiO2 (in the case of CF4). This fluorocarbon film prevents the etching of Si and SiO2 by atomic F. However, a similar effect is not usually observed for Si3N4 due to the method of deposit generation.

Lee et al.[24] found that etching selectivity could be controlled by adjusting the thickness of the fluorocarbon film and the flow rate of CH4 gas. With reference [24] it was also found that the etching selectivity could be controlled by adjusting the thickness of the fluorocarbon film and the flow rate of CH4 gas. The increase in carbon content in the fluorocarbon film with the increase in CH4 gas leads to a decrease in the etching rate of the silicon oxide and silicon nitride films, ultimately leading to an etching stop.

These sources suggest that specific gas compositions, namely Ar/CF4/O2, Ar/CF4/N2, and Ar/CF4/H2 formulations, can achieve the desired etching selectivity. Using the capabilities of the current MIP equipment, we used a variety of gas combinations including Ar (argon), CF4 (tetrafluoromethane), O2 (oxygen), and H2 (hydrogen). In addition, N2 (nitrogen) was introduced as a new etching gas for experimental studies.

These gas compositions were strategically selected based on their efficacy in achieving etching selectivity for the material of interest. Different gas combinations allow the manipulation of plasma chemistry, energy levels, and interaction mechanisms during the etching process. This, in turn, facilitates

the targeted removal of specific materials while maintaining the integrity of other materials to achieve the desired etching selectivity.

By utilising these established gas formulations and combining a variety of etching gases, our research efforts are dedicated to discovering the optimal conditions to facilitate the desired etching selectivity between polysilicon, silicon nitride, silicon dioxide and other materials. This approach utilises the versatility of the MIP equipment to systematically explore and identify the most effective gas compositions to achieve our desired etch results.

4.3. MIP Afterglow Etching

In pursuing material etching selectivity, we recognise the importance of obtaining comprehensive data on the etch rates of individual materials. To address this aspect, we performed a series of dedicated etch experiments for each material and maintained uniform experimental parameters across all experiments. This included input power, microwave frequency, and etch time, the only variable being the gas composition used.

The input power was consistently set to 30 W throughout the experiments to ensure consistency in the energy supplied. The selected microwave frequency was fixed at 2430 MHz to provide a coordinated condition for reliable comparisons. In addition, a fixed etching time was used, but this was adjusted for some particularly thin materials.

After the etching process, we turned to the Dektak Stylus Profiler, a precision instrument capable of quickly and accurately measuring the height of surface features to within 10 nanometres of ultra-high accuracy.

This section describes the results of different gas formulations, each of which holds valuable insights. We have taken a close look at the shape of the etched contours, assessed the width and depth dimensions of the resulting features, and carefully evaluated the overall volume of the etched area. By carefully analysing these results, we aim to gain a comprehensive understanding of the etching behaviour under different gas compositions, thus achieving the overall goal of our research work.

4.3.1. Ar/CF4/O2 Plasma Etching

In the Ar/CF4/O2 plasma etching process, argon is the carrier gas, and CF4 is the main etching gas. The F atoms and CF3 radicals generated by CF4 decomposition react with the material surface. Introducing oxygen (O2) can significantly improve the etching rate of the material. The decomposition of oxygen in the plasma produces oxygen ions and oxygen radicals, which readily oxidise the material's surface, thus accelerating the etching process. Reference [20] states that the addition of O2 also helps to achieve selectivity between Si and SiO2, so Ar/CF4/O2 was chosen as the initial formulation for the study.

During the experiments, the flow rate of the carrier gas argon was kept at 1400 sccm, and the combined flow rate of CF4 and O2 was maintained at 10 sccm. The concentrations of CF4 and O2 were

varied at nine different etching points. The etching profiles of the three materials at different ratios are shown in Fig.4.1. When the concentration of CF4 is significantly higher than that of O2, the etching curves show a spherical cap shape. As the concentration of O2 increases, the etching curve gradually transitions to a more conical shape.

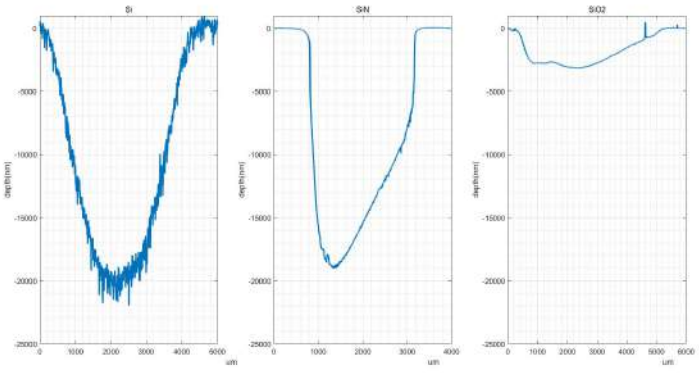

Figure 4.1: Profiles of Si, SiO2, Si3N4 etching with the same recipe (20% O2)

Tab.4.1 summarises the results of the etching experiments. In all tables of selectivity data, bold data is the optimal selectivity and italic data is the optimal reverse selectivity. The results show that the etching rate of Si3N4 is the highest, followed by Si, while the etching rate of SiO2 is still relatively low. As the O2 content increases, the etching rate increases significantly. At 30% O2, the etching rates of all materials reached a maximum. However, as the oxygen concentration increases, the etching rate decreases gradually. This experiment demonstrates how controlling the amount of oxygen added during the Ar/CF4/O2 plasma etching process significantly affects the etching rate and selectivity of the various materials, affecting their etching profiles and overall etching efficiency.

Table 4.1: Etching results of Si, SiO2, Si3N4 materials by Ar/CF4/O2 plasma

Bold data: optimal selectivity, italic data: optimal reverse selectivity

Gas Flow (fixed 10sccm)				Power (W)	Relative Etch Rate			Etch selectivity		
Ar	O2	CF4	N2		PECVD SiO2	PECVD Si3N4	Si	Si3N4/ SiO2	Si3N4/ Si	Si/ SiO2
1400	0	10	0	30	0.101	0.064	0.706	***0.63***	***0.09***	6.99
1400	0.5	9.5	0	30	0.316	2.52	1.84	7.97	1.37	5.82
1400	1	9	0	30	0.338	3.52	2.76	**10.41**	1.28	**8.17**
1400	2	8	0	30	0.608	4.74	3.5	7.8	1.35	5.76
1400	3	7	0	30	0.694	4.76	3.3	6.86	1.44	4.76
1400	5	5	0	30	0.564	4.02	1.6	7.13	2.51	2.84
1400	7	3	0	30	0.27	2.76	0.38	10.22	**7.26**	1.41
1400	9	1	0	30	0.122	0.3	0	2.46	High	***0***
1400	10	0	0	30	0.06	0.1	0.049	1.67	2.04	0.82

4.3.2. Ar/CF4/N2 Plasma Etching

After an initial review of the literature, [21, 22] agree that the addition of N2 significantly increases the etching rate of silicon nitride. Several hypotheses have been proposed to elucidate this interesting phenomenon:

Kastenmeier et al.[22] proposed that N2 undergoes ionisation to produce nitrogen ions, which react with oxygen in the ambient air to form NO (nitric oxide). It has been frequently observed that NO significantly increases the rate of CF4 etching on nitride materials. Under certain circumstances, the controlled introduction of moderate amounts of NO gas can stimulate surface reactions during the etching process, thereby increasing the etching rate of silicon nitride. Because of this, N2 is considered a gas with the potential to achieve etching selectivity. For this reason, an Ar/CF4/N2 plasma formulation was used for the experimental studies in this section. Consistent with previous experiments, the flow rate of the carrier gas (Argon) was held constant at 1400 sccm, while the combined flow rate of CF4 and N2 was held steady at 10 sccm. Variations in CF4 and N2 concentrations were explored at nine different etch points.

Tab.4.2 briefly summarises the results of the etching experiments. Consistent with the results of previous studies, Si3N4 has the highest etching rate, followed by Si, while SiO2 has the lowest etching rate. The etching rate of Si3N4 increased slightly with the increase of N2 content. When the nitrogen content reaches 30%, the etching rates of Si3N4 all reach peak value. The subsequent increase in nitrogen concentration leads to a gradual decrease in the etching rate.

Comparing the etching curves, it can be found that the etching results of CF4 + N2 are similar to those of CF4 + O2. However, a noteworthy difference in the etching rate occurs. Unlike the observed significant enhancement of the etching by O2, the addition of N2 to CF4 has a relatively limited effect

Table 4.2: Etching results of Si, SiO2, Si3N4 materials by Ar/CF4/N2 plasma
Bold data: optimal selectivity, italic data: optimal reverse selectivity

Gas Flow (fixed 10sccm)				Power (W)	Relative Etch rate			Etch selectivity		
Ar	O2	CF4	N2		PECVD SiO2	PECVD Si3N4	Si	Si3N4/ SiO2	Si3N4/ Si	Si/ SiO2
1400	0	10	0	30	0.101	0.064	0.706	***0.63***	***0.09***	6.99
1400	0	9.5	0.5	30	0.108	0.15	0.78	1.39	0.19	7.22
1400	0	9	1	30	0.106	1.17	0.82	11.04	1.43	7.74
1400	0	8	2	30	0.104	1.19	0.84	11.44	1.42	8.08
1400	0	7	3	30	0.096	1.338	0.82	**13.94**	**1.63**	**8.54**
1400	0	5	5	30	0.194	1.12	0.806	5.77	1.39	4.15
1400	0	3	7	30	0.193	0.82	0.808	4.25	1.01	4.19
1400	0	1	9	30	0.212	1.9	0.46	8.96	4.13	***2.17***
1400	0	0	10	30	0	0	0	0	0	0

on the etching rate. This observation suggests that the selectivity of N2 for etching is fairly consistent across the three materials and that the addition of N2 has little effect on etch rate and etching selectivity.

4.3.3. Ar/CF4/H2 Plasma Etching

Through a comprehensive review of the literature[23], it has been found that adjusting the ratio of hydrogen (H2) in an Ar/CF4 plasma can produce varying degrees of etching selectivity. When an Ar/CF4 plasma is introduced, hydrogen and fluorine gas from CF4 decomposition undergo a chemical change in the plasma environment. This reaction culminates in the formation of hydrofluoric acid (HF). This highly corrosive acid readily comes into contact with the surface of the etched material, thereby triggering the start of the etching process.

The reaction with hydrofluoric acid is of particular importance in the case of materials such as silicon (Si), silicon dioxide (SiO2), and silicon nitride (Si3N4), where HF reacts with the surfaces of these materials to effectively catalyse and accelerate the etching process. This mechanism establishes a link between the addition of H2 and an increase in the etching rate.

However, introducing H2 into the Ar/CF4 plasma triggers a worrisome weakness - once H2 is added, the plasma is easily off. Given this unexpected plasma instability, the etching conditions were adjusted to ensure plasma stability. While the carrier gas (argon) remained unchanged at 1400 sccm, it was now delivered as a mixture of 1100 sccm pure argon and 300 sccm of 2% H2. The flow rate of the H2 was set precisely at 6 sccm. Despite these changes, all other etching conditions were strictly maintained.

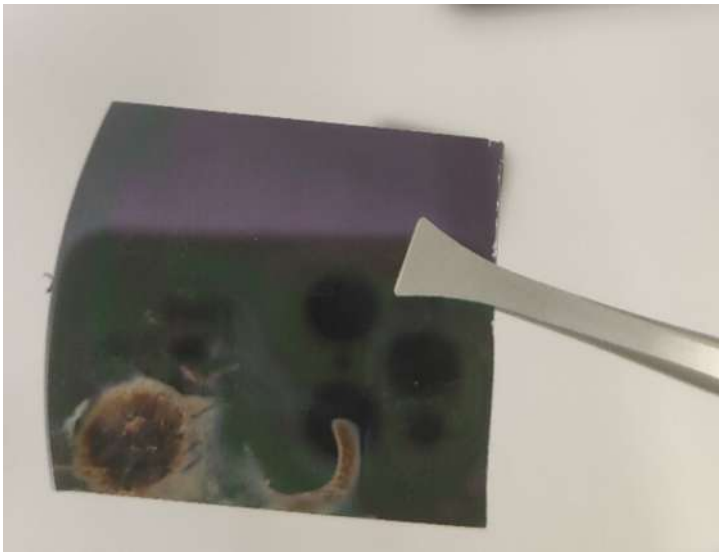

Figure 4.2: SiO2 sample after Ar/CF4/H2 Plasma Etching

As a result of these efforts, the results of the Ar/CF4/H2 etching are shown in Fig.**??**. We found an apparent and exciting phenomenon - a layer of black material was deposited on the material's surface, where the etching was not supposed to occur. This phenomenon persisted in all three materials where etching was performed. Strikingly, this finding suggests that introducing H2 resulted in the deposition of unwanted material on the surface instead of producing the expected etching results.

These experimental results exemplify the complexity of plasma-based processes and the complications that can result from introducing additional gases. At low enough H2 concentrations, a thin fluorocarbon film forms on the surface of the material during etching. The film formed on the surface is the same for the three materials, indicating that whether such a film forms is determined by the concentration of reactants reaching the surface from the gas phase rather than by the properties of the material surface.

Marra et al. [25] explains the reason for the deposition of black material may be due to in CF4/H2 plasma, the structure of the fluorocarbon layer is mainly affected by the relative fluxes of F and H incident on the surface. H and F participate in competition for surface sites, and in H-rich plasmas, H tends to extract and displace F on the surface and interior of the fluorocarbon film. In contrast, in F-rich plasmas, F can extract and displace H.

4.4. Temperature Effect

In our previous experiments, the addition of N2 along with H2 showed limited improvement in achieving the desired etching selectivity. This prompted us to explore other ways to influence etching selectivity, and temperature became a compelling variable for several reasons.

Firstly, the temperature at which a sample surface is etched can significantly affect the chemical reaction rate and even change the reaction mechanism. These changes can affect the etch rates of different materials and the overall etching selectivity.[26] Secondly, the advantage of controlling the

sample temperature within the MIP machines is that it is relatively easy to do so by splitting the etching time into multiple cycles. For example, the previous of continuous etching test can be divided into multiple cycles of with a shorter etching duration in each cycle, allowing enough time for the sample to cool between cycles. This method is effective in controlling temperature variations during the etching process. Finally, previous experience has shown that temperature control can effectively affect etching selectivity, which prompted us to explore its potential in this experiment.

Table 4.3: Etching results of Si, SiO2, Si3N4 materials at different temperatures

Bold data: optimal selectivity, italic data: optimal reverse selectivity

Gas Flow (fixed 10sccm)			Power(W)	Relative Etch rate					
				One continuous long duration etch cycle (High Temperature)			Multiple cycles with a shorter etching duration (Low Temperature)		
Ar	O2	CF4		PECVD SiO2	PECVD Si3N4	Si	PECVD SiO2	PECVD Si3N4	Si
1400	0	10	30	0.101	0.064	0.706	0.056	0	0.394
1400	0.5	9.5	30	0.316	2.52	1.84	0.208	0.16	1.392
1400	1	9	30	0.338	3.52	2.76	0.318	0.406	2.154
1400	2	8	30	0.608	4.74	3.5	0.574	5.02	3.594
1400	3	7	30	0.694	4.76	3.3	0.68	4.36	3.606
1400	5	5	30	0.564	4.02	1.6	0.45	4.5	1.704
1400	7	3	30	0.27	2.76	0.38	0.304	0.626	0.834
1400	9	1	30	0.122	0.3	0	0.082	0.732	0
1400	10	0	30	0.06	0.1	0.049	0	0	0
Gas Flow (fixed 10sccm)			Power(W)	Etch selectivity					
				One continuous long duration etch cycle (High Temperature)			Multiple cycles with a shorter etching duratiom (Low Temperature)		
Ar	O2	CF4		Si3N4/ SiO2	Si3N4/ Si	Si/ SiO2	Si3N4/ SiO2	Si3N4/ Si	Si/ SiO2
1400	0	10	30	0.63	0.09	6.99	0	0	7.04
1400	0.5	9.5	30	7.97	1.37	5.82	***0.77***	***0.11***	6.69
1400	1	9	30	**10.41**	***1.28***	**8.17**	1.28	0.19	**6.77**
1400	2	8	30	7.8	1.35	5.76	8.75	1.4	6.26
1400	3	7	30	6.86	1.44	4.76	6.41	1.21	5.3
1400	5	5	30	7.13	2.51	2.84	**10**	**2.64**	3.79
1400	7	3	30	10.22	**7.26**	1.41	2.06	0.75	***2.74***
1400	9	1	30	***2.46***	High	0	8.93	High	0
1400	10	0	30	1.67	2.04	0.82	0	0	0

In the temperature-affected experiments, we kept all other conditions strictly unchanged. The only change was to split the etching time, which is a continuous etching, into multiple cycles with a shorter etching duration in each cycle. The results of the experiment are shown in Tab.4.3, where the etch rates and corresponding etching selectivity results at different temperatures are compared side by side.

A closer look at these results reveals a clear pattern - the etching rate decreases with temperature for all three materials compared to higher temperatures. Notably, specific etching conditions - high CF4 ratio and low O2 ratio - show significant differences in etching rates. At low temperatures, the etch rate of Si3N4 decreases dramatically, the etching rate of Si decreases slightly, and the etch rate of SiO2 remains almost constant.

This observation is potentially significant. At low temperatures and specific gas compositions, the etching selectivity can be controlled to reverse the Si3N4/SiO2 etch dynamics. This means it is possible to selectively etch SiO2 without affecting Si3N4 or to etch Si without affecting Si3N4.

This novel approach to temperature regulation emphasises the intricate interplay between external variables and etching selectivity. The etching selectivity we need is achieved by using temperature as a regulating factor.

4.5. MIP Afterglow Etching Selectivity Between Si/SiO2/Si3N4

While the etching rates of various materials are vital data points to guide future work, our primary goal in these experiments was not just numerical. Instead, we sought to reveal the complex etching selectivity between three different materials: silicon (Si), silicon dioxide (SiO2), and silicon nitride (Si3N4). This quest delves into the precise formulations and conditions that facilitate the emergence of selective etching behaviour, embodying the essence of our research.

This part of our research focuses on exploring the pairwise selectivity dynamics of these three materials. We aim to scrutinise how specific etching recipes cause one material to be etched in preference to the other, thereby demonstrating the power of tailored plasma conditions in designing controlled material removal.

As the experiments yielded compelling results, we endeavored to elucidate formulations that hold promise for achieving etching selectivity. These recipes are a practical manifestation of our intent - to exploit subtle differences in plasma chemistry, gas composition, and power dynamics to achieve a delicate balance between etch rate and selectivity, resulting in precise and delicate sculpting of materials.

4.5.1. Selectivity Between Si/SiO2

The experimental results highlight the significant impact of varying the ratio of CF4 to O2 in an Ar/CF4/O2 plasma etching environment. Effective control of this ratio allows for precise control of etching selectivity and even reversal of the selectivity relationship. Specifically, the performance of Si/SiO2 etching selectivity is particularly interesting.

By analysing the experimental results in Tab.4.6, it is clear that the highest etching selectivity between Si and SiO2 is achieved when the oxygen ratio in the plasma mixture is set at 10%. This particular gas composition maximises the difference in etch rates between silicon and silica, thus providing the most favourable conditions for selectively etching one material while the other remains largely unaffected.

In contrast, when the oxygen ratio was adjusted to 90%, the silicon/silicon dioxide etching selectivity was significantly reversed. This indicates a change in the etch rates of silicon and silica, with silicon etching preferentially over silica. This dynamic change highlights the intricate interactions between CF4 and O2 gases and the inherent material properties and reaction mechanisms.

4.5.2. Selectivity Between Si3N4/Si

At the same time, exploring etching selectivity between silicon (Si) and silicon nitride (Si3N4) involves an in-depth study of the tuning of CF4 to O2 ratios in the Ar/CF4/O2 plasma etching environment. The dynamic interactions between these gases are a powerful tool for shaping the etch properties of these materials, providing a complex pathway for achieving accurate etching selectivity results.

Upon closely examining the experimental results in Tab.4.8, we have discovered a striking phenomenon: the etching selectivity between Si3N4 and Si responds profoundly to changes in the CF4 to O2 ratio. Notably, the etching selectivity reaches its lowest point when the plasma mixture consists entirely of CF4 gas. In contrast, a critical turning point occurs when the oxygen ratio is fine-tuned to about 70%. At this particular gas composition, the selectivity between Si3N4 and Si changes dramatically.

Interestingly, temperature is also a determining factor in the selectivity of Si/Si3N4 etching. The lower the temperature, the lower the etch rate of Si3N4, while the etching rate of Si decreases only slightly. Therefore, this effect contributes to the Si/Si3N4 etching selectivity under certain circumstances. In particular, when the etching process is performed at lower temperatures and high CF4 concentrations, the ability to etch Si is enhanced without unduly affecting Si3N4.

4.5.3. Selectivity Between SiO2/Si3N4

Finally, we discuss the etching selectivity of SiO2 versus Si3N4. In Ar/CF4/O2 plasma etching, the adjustment of the ratio of CF4 to O2 causes significant changes in the etch characteristics of both silicon nitride (Si3N4) and silicon dioxide (SiO2) materials.

After careful analysis of the experimental data in Tab.4.7, a clear pattern was found - a delicate balance was achieved by adjusting the ratio of CF4 to O2, resulting in etching selectivity between Si3N4 and SiO2. Remarkably, the etching selectivity between silicon nitride and silicon dioxide is minimised when the mixed plasma consists of only CF4 gas. On the contrary, with the gradual increase of oxygen content in the plasma environment, the etching rate of Si3N4 increases dramatically, and the selectivity between Si3N4 and Si undergoes a significant reversal. This is evidenced by a marked shift in the emphasis of the etching process from SiO2 to Si3N4, with the etching selectivity between Si3N4 and SiO2 peaking when the oxygen ratio is precisely adjusted to 10%.

The role of temperature is equally important and needs to be clarified. At lower temperatures, the etch rate of Si3N4 drops dramatically, while the etch rate of SiO2 remains very stable. This unique thermal behaviour yields an intriguing result: under pure CF4 or predominantly CF4-rich mixtures (90% CF4), there is a clear inversion of the etching selectivity between Si/Si3N4. Therefore, if the goal is to selectively etch SiO2 without affecting Si3N4, skilfully executed high CF4 concentration etching at low temperatures becomes a prerequisite.

4.5.4. Comparison of PECVD and LPCVD Materials

We conclude this chapter by comprehensively comparing two widely used thin film deposition techniques - plasma enhanced chemical vapour deposition (PECVD) and low-pressure chemical vapour deposition (LPCVD). Both methods are critical in microelectronics manufacturing, providing a means of depositing necessary thin film materials on semiconductor devices. It is essential to clarify the differences between the two, centred around deposition pressure and the underlying growth mechanisms of the materials.

LPCVD is an acronym for Low-Pressure Chemical Vapor Deposition and operates at relatively low air pressures, typically in the range of tens to hundreds of Pascals. This method dissociates precursor molecules in the chemical vapour phase into reactants at reduced pressure. These reactants are then sensibly deposited onto the substrate surface. The inherent advantage of LPCVD is the ability to produce higher quality, more homogeneous materials. This process has complex effects on the resulting material's deposition rate and compositional homogeneity.[27]

In contrast, PECVD (Plasma Enhanced Chemical Vapour Deposition) involves deposition in a plasma-rich environment characterised by increased gas pressure, typically ranging from a few hundred to a few thousand Pascals. The key to this technique is the activation of gas molecules in the plasma to form energetic ions and reactive seeds. These components, in turn, coordinate the deposition of the target material. PECVD technology, whilst accelerating the deposition rate, also introduces residual stresses and impurities into the deposited material.[28]

Materials generated by LPCVD tend to have a more compact and dense structural configuration than PECVD. As a result, LPCVD-generated materials are generally more resistant to etching. The experimental results in Tab.4.4 further support this assumption as they consistently emphasise that the etching rates of LPCVD-generated SiO2 and Si3N4 are essentially lower than those of similar materials generated by PECVD. This apparent difference in etch rate also leads to different etching selectivity for materials with varying deposition methods. The difference in selectivity can be seen in Tab. 4.5.

These findings highlight the importance of clarifying the deposition method employed before formulating the appropriate etching recipe.

Table 4.4: Etching rates of LPCVD and PECVD materials

Gas Flow (fixed 10sccm)			Power (W)	Relative Etch rate				
Ar	O2	CF4		PECVD SiO2	PECVD Si3N4	Si	LPCVD SiO2	LPCVD Si3N4
1400	0	10	30	0.101	0.064	0.706	0.7	0.92
1400	0.5	9.5	30	0.316	2.52	1.84	0.28	2.46
1400	1	9	30	0.338	3.52	2.76	0.5	1.444
1400	2	8	30	0.608	4.74	3.5	0.65	3.06
1400	3	7	30	0.694	4.76	3.3	0.85	2.14
1400	5	5	30	0.564	4.02	1.6	0.5	2.08
1400	7	3	30	0.27	2.76	0.38	0.35	1.27
1400	9	1	30	0.122	0.3	0	0.14	0.16
1400	10	0	30	0.06	0.1	0.049	0	0

Table 4.5: Etching selectivity of LPCVD and PECVD materials

Bold data: optimal selectivity, italic data: optimal reverse selectivity

Gas Flow (fixed 10sccm)			Power (W)	Etch selectivity					
Ar	O2	CF4		Si3N4/SiO2 (PECVD)	Si3N4 (PECVD)/Si	Si/SiO2 (PECVD)	Si3N4/SiO2 (LPCVD)	Si3N4 (LPCVD)/Si	Si/SiO2 (LPCVD)
1400	0	10	30	0.63	0.09	6.99	1.31	1.3	1.01
1400	0.5	9.5	30	7.97	1.37	5.82	8.79	1.34	6.57
1400	1	9	30	10.41	1.28	8.17	2.89	0.52	5.52
1400	2	8	30	7.8	1.35	5.76	4.71	0.87	5.38
1400	3	7	30	6.86	1.44	4.76	2.52	0.65	3.88
1400	5	5	30	7.13	2.51	2.84	4.16	1.3	3.2
1400	7	3	30	10.22	7.26	1.41	3.63	3.34	1.09
1400	9	1	30	2.46	High	0	1.14	High	0
1400	10	0	30	1.67	2.04	0.82	0	0	0

4.6. Conclusion

The experiments detailed in this chapter were carried out using a MIP machine based on CF4 gas, and the primary purpose was to study the etching selectivity between silicon (Si), silicon dioxide (SiO2), and silicon nitride (Si3N4) Material. The experimental design and parameters were developed based on a thorough review of the existing literature and knowledge gained from previous studies.

It was concluded from the experimental results that the introduction of CF4/O2 gas mixture into the MIP system achieved acceptable results in terms of etching selectivity between these different materials. The CF4/O2 gas composition effectively achieved the desired material-specific etch, demonstrating the importance of the gas formulation in this process.

Furthermore, temperature experiments performed in parallel revealed that temperature also plays a crucial role in influencing the etching properties of these materials.

Table 4.6: Selectivity between Si/SiO2

Bold data: optimal selectivity, italic data: optimal reverse selectivity

Gas Flow (fixed 10sccm)				Power (W)	Etch time	Selectivity of Si/SiO2
Ar	O2	CF4	N2			
1400	0	10	0	30	One continuous long etching cycle	*6.99*
1400	0.5	9.5	0	30	One continuous long etching cycle	*5.82*
1400	1	9	0	30	One continuous long etching cycle	**8.17**
1400	2	8	0	30	One continuous long etching cycle	**5.76**
1400	3	7	0	30	One continuous long etching cycle	4.76
1400	5	5	0	30	One continuous long etching cycle	**2.84**
1400	7	3	0	30	One continuous long etching cycle	**1.41**
1400	9	1	0	30	One continuous long etching cycle	*0*
1400	10	0	0	30	One continuous long etching cycle	0.82
1400	0	10	0	30	One continuous long etching cycle	*6.99*
1400	0	9.5	0.5	30	One continuous long etching cycle	*7.22*
1400	0	9	1	30	One continuous long etching cycle	7.74
1400	0	8	2	30	One continuous long etching cycle	**8.08**
1400	0	7	3	30	One continuous long etching cycle	**8.54**
1400	0	5	5	30	One continuous long etching cycle	**4.15**
1400	0	3	7	30	One continuous long etching cycle	**4.19**
1400	0	1	9	30	One continuous long etching cycle	***2.17***
1400	0	0	10	30	One continuous long etching cycle	0
1400	0	10	0	30	Multiple short etching cycles	*7.04*
1400	0.5	9.5	0	30	Multiple short etching cycles	*6.69*
1400	1	9	0	30	Multiple short etching cycles	6.77
1400	2	8	0	30	Multiple short etching cycles	**6.26**
1400	3	7	0	30	Multiple short etching cycles	**5.3**
1400	5	5	0	30	Multiple short etching cycles	**3.79**
1400	7	3	0	30	Multiple short etching cycles	2.74
1400	9	1	0	30	Multiple short etching cycles	*0*
1400	10	0	0	30	Multiple short etching cycles	0

Table 4.7: Selectivity between SiO2/Si3N4

Bold data: optimal selectivity, italic data: optimal reverse selectivity

Gas Flow (fixed 10sccm)				Power (W)	Etch time	Selectivity of Si3N4/SiO2
Ar	O2	CF4	N2			
1400	0	10	0	30	One continuous long etching cycle	*0.63*
1400	0.5	9.5	0	30	One continuous long etching cycle	7.97
1400	1	9	0	30	One continuous long etching cycle	**10.41**
1400	2	8	0	30	One continuous long etching cycle	7.8
1400	3	7	0	30	One continuous long etching cycle	6.86
1400	5	5	0	30	One continuous long etching cycle	7.13
1400	7	3	0	30	One continuous long etching cycle	10.22
1400	9	1	0	30	One continuous long etching cycle	2.46
1400	10	0	0	30	One continuous long etching cycle	1.67
1400	0	10	0	30	One continuous long etching cycle	*0.63*
1400	0	9.5	0.5	30	One continuous long etching cycle	1.39
1400	0	9	1	30	One continuous long etching cycle	11.04
1400	0	8	2	30	One continuous long etching cycle	11.44
1400	0	7	3	30	One continuous long etching cycle	**13.94**
1400	0	5	5	30	One continuous long etching cycle	5.77
1400	0	3	7	30	One continuous long etching cycle	4.25
1400	0	1	9	30	One continuous long etching cycle	8.96
1400	0	0	10	30	One continuous long etching cycle	0
1400	0	10	0	30	Multiple short etching cycles	0
1400	0.5	9.5	0	30	Multiple short etching cycles	*0.77*
1400	1	9	0	30	Multiple short etching cycles	1.28
1400	2	8	0	30	Multiple short etching cycles	**8.75**
1400	3	7	0	30	Multiple short etching cycles	6.41
1400	5	5	0	30	Multiple short etching cycles	10
1400	7	3	0	30	Multiple short etching cycles	2.06
1400	9	1	0	30	Multiple short etching cycles	8.93
1400	10	0	0	30	Multiple short etching cycles	0

Table 4.8: Selectivity between Si3N4/Si

Bold data: optimal selectivity, italic data: optimal reverse selectivity

Gas Flow (fixed 10sccm)				Power (W)	Etch time	Selectivity of Si3N4/Si
Ar	O2	CF4	N2			
1400	0	10	0	30	One continuous long etching cycle	*0.09*
1400	0.5	9.5	0	30	One continuous long etching cycle	*1.37*
1400	1	9	0	30	One continuous long etching cycle	**1.28**
1400	2	8	0	30	One continuous long etching cycle	**1.35**
1400	3	7	0	30	One continuous long etching cycle	1.44
1400	5	5	0	30	One continuous long etching cycle	**2.51**
1400	7	3	0	30	One continuous long etching cycle	**7.26**
1400	9	1	0	30	One continuous long etching cycle	High
1400	10	0	0	30	One continuous long etching cycle	2.04
1400	0	10	0	30	One continuous long etching cycle	*0.09*
1400	0	9.5	0.5	30	One continuous long etching cycle	*0.19*
1400	0	9	1	30	One continuous long etching cycle	1.43
1400	0	8	2	30	One continuous long etching cycle	**1.42**
1400	0	7	3	30	One continuous long etching cycle	**1.63**
1400	0	5	5	30	One continuous long etching cycle	**1.39**
1400	0	3	7	30	One continuous long etching cycle	**1.01**
1400	0	1	9	30	One continuous long etching cycle	**4.13**
1400	0	0	10	30	One continuous long etching cycle	0
1400	0	10	0	30	Multiple short etching cycles	*0*
1400	0.5	9.5	0	30	Multiple short etching cycles	*0.11*
1400	1	9	0	30	Multiple short etching cycles	0.19
1400	2	8	0	30	Multiple short etching cycles	**1.4**
1400	3	7	0	30	Multiple short etching cycles	**1.21**
1400	5	5	0	30	Multiple short etching cycles	**2.64**
1400	7	3	0	30	Multiple short etching cycles	0.75
1400	9	1	0	30	Multiple short etching cycles	High
1400	10	0	0	30	Multiple short etching cycles	0

5

Conclusion

5.1. Summary

This thesis describes the experiments and their results around optimising the MIP machine. The experiments are divided into two parts in total, improved cavity and CF4-based MIP machine etching selectivity experiments.

Chapter 3 focuses on the idea of the improved cavity. Regarding experimental results, the higher Beenakker cavity has not significantly improved the etching efficiency of the system as initially expected. However subsequent experiments demonstrated that the improved cavity design could generate a stable plasma sustainably at higher input power levels.

The experiments detailed in Chapter 4 were conducted using a CF4-based MIP machine with the main objective of investigating the etching selectivity between Silicon (Si), Silicon oxide (SiO2), and Silicon Nitride (Si3N4) materials. The results show that the CF4/O2 gas recipe is effective in achieving etching selectivity and that temperature is also a critical factor in these etching selectivities.

5.2. Future Work

5.2.1. Potential for High Power MIP Machines

Based on the experimental results of chapter 3, the modified Beenakker cavity can produce stable plasma at high input power. In this case, the high-power MIP machines provide a possible method. The high input power will undoubtedly have a significant increase in etching efficiency.

5.2.2. Etching Experiment of SiC

Depending on the specific industrial requirements, the target materials for etching also include mixtures of silicon nitride (Si3N4) and silicon carbide (SiC). Therefore, it is essential to focus not only on the etch rate of Si3N4 but also to delve deeper into the etch rate of SiC.

Therefore, future research efforts include exploring the etching efficiency of SiC and delving into the etching selectivity of SiC with other materials. These combined efforts will ultimately lead to a more complete understanding of the etching processes involved, leading to the development of customised etching solutions that meet the specific requirements of Si3N4 and SiC mixtures.

References

[1] Jiaqi Tang, J. Schelen, and C. Beenakker. "Plasma Etching for Failure Analysis of Integrated Circuit Packages". In: *Journal of Cheminformatics - J Cheminf* 34 (Mar. 2011). DOI: 10.1149/1.3567691.

[2] Jiaqi Tang. *MIP decapsulation of Cu and Ag Wire IC Package*. 2021. URL: https://jiaco-instruments.com/decapsulation-technology/.

[3] Jiaqi Tang and C. Beenakker. "MIP Plasma Decapsulation of Copper-wired Semiconductor Devices for Failure Analysis". In: (Jan. 2014). DOI: https://doi.org/10.4233/uuid:1069e3a0-90bc-46e3-8727-69d96107cc61.

[4] N. Rait, D.W. Golightly, and C.J. Massoni. "An improved Beenakker-type cavity for microwave induced plasma spectrometry". In: *Spectrochimica Acta Part B: Atomic Spectroscopy* 39.7 (1984), pp. 931–937. ISSN: 0584-8547. DOI: https://doi.org/10.1016/0584-8547(84)80109-3. URL: https://www.sciencedirect.com/science/article/pii/0584854784801093.

[5] SAIREM. *SAIREM Industrial Microwave Generators*. 2022. URL: https://www.sairem.com/industrial-microwave-generators/.

[6] Krzysztof Jankowski and Edward Reszke. "Microwave induced plasma analytical spectrometry". In: *RSC Analytical Spectroscopy Series* 12 (Jan. 2011), pp. 1–263.

[7] C.I.M. Beenakker. "A cavity for microwave-induced plasmas operated in helium and argon at atmospheric pressure". In: *Spectrochimica Acta Part B: Atomic Spectroscopy* 31.8 (1976), pp. 483–486. ISSN: 0584-8547. DOI: https://doi.org/10.1016/0584-8547(76)80047-X. URL: https://www.sciencedirect.com/science/article/pii/058485477680047X.

[8] C.I.M. Beenakker, Bieneke Bosman, and P.W.J.M. Bousman. "An assessment of a microwave-induced plasma generated in argon with a cylindrical TM010 cavity as an excitation source for emission spectrometric analysis of solutions". In: *Spectrochimica Acta Part B: Atomic Spectroscopy* 33.7 (1978), pp. 373–381. ISSN: 0584-8547. DOI: https://doi.org/10.1016/0584-8547(78)80015-9. URL: https://www.sciencedirect.com/science/article/pii/0584854778800159.

[9] X Yang, S E Babayan, and R F Hicks. "Measurement of the fluorine atom concentration in a carbon tetrafluoride and helium atmospheric-pressure plasma". In: *Plasma Sources Science and Technology* 12.3 (July 2003), p. 484. DOI: 10.1088/0963-0252/12/3/325. URL: https://dx.doi.org/10.1088/0963-0252/12/3/325.

[10] Jiaqi Tang et al. "Fast Etching of Molding Compound by an Ar/O2/CF4 Plasma and Process Improvements for Semiconductor Package Decapsulation". In: *ECS Journal of Solid State Science and Technology* 1 (Aug. 2012), P175–P178. DOI: 10.1149/2.019204jss.

[11] C Mogab, A Adams, and Daniel Flamm. "Plasma Etching of Si and SiO2—The Effect of Oxygen Additions to CF4 Plasmas". In: *Journal of Applied Physics* 49 (Aug. 1978), p. 3796. DOI: 10.1063/1.325382.

[12] C. I. M. Beenakker, J. H. J. van Dommelen, and R. P. J. van de Poll. "Decomposition and product formation in CF4-O2 plasma etching silicon in the afterglow". In: *Journal of Applied Physics* 52.1 (Jan. 1981), pp. 480–485. ISSN: 0021-8979. DOI: 10.1063/1.329812. eprint: https://pubs.aip.org/aip/jap/article-pdf/52/1/480/7971457/480_1_online.pdf. URL: https://doi.org/10.1063/1.329812.

[13] Hewlett-Packard Company. Microwave Division and I.L. Kosow. *Microwave Theory and Measurements*. Prentice-Hall, 1962. URL: https://books.google.nl/books?id=TgNTAAAAMAAJ.

[14] Yassine Kabouzi et al. "Radial Contraction of Microwave-Sustained Plasma Columns at Atmospheric Pressure". In: *Journal of Applied Physics* 91 (Feb. 2002), pp. 1008–1019. DOI: 10.1063/1.1425078.

[15] Vincent Donnelly. "Review Article: Reactions of fluorine atoms with silicon, revisited, again". In: *Journal of Vacuum Science & Technology A: Vacuum, Surfaces, and Films* 35 (Sept. 2017), p. 05C202. DOI: 10.1116/1.4983922.

[16] M. Morita et al. "Growth of native oxide on a silicon surface". In: *Journal of Applied Physics* 68.3 (Aug. 1990), pp. 1272–1281. ISSN: 0021-8979. DOI: 10.1063/1.347181. eprint: https://pubs.aip.org/aip/jap/article-pdf/68/3/1272/10575271/1272_1_online.pdf. URL: https://doi.org/10.1063/1.347181.

[17] Sanborn C. Brown. *Basic data of plasma physics: The fundamental data on electrical discharges in gases*. Technology Press of MIT, 1959.

[18] C Mogab, A Adams, and Daniel Flamm. "Plasma Etching of Si and SiO2—The Effect of Oxygen Additions to CF4 Plasmas". In: *Journal of Applied Physics* 49 (Aug. 1978), p. 3796. DOI: 10.1063/1.325382.

[19] Jiaqi Tang, J.B.J. Schelen, and C.I.M. Beenakker. "Process control in plasma decapsulation: Preventing damage to the copper wire bonds & controlled removal of Si3N4 passivation layer". In: Aug. 2012, pp. 1194–1199. ISBN: 978-1-4673-1682-8. DOI: 10.1109/ICEPT-HDP.2012.6474821.

[20] Lee M. Loewenstein. "Effect of oxygen on fluorine-based remote plasma etching of silicon and silicon dioxide". In: *Journal of Vacuum Science & Technology A* 6.3 (May 1988), pp. 1984–1988. ISSN: 0734-2101. DOI: 10.1116/1.575221. eprint: https://pubs.aip.org/avs/jva/article-pdf/6/3/1984/11941919/1984_1_online.pdf. URL: https://doi.org/10.1116/1.575221.

[21] M. G. Blain, T. L. Meisenheimer, and J. E. Stevens. "Role of nitrogen in the downstream etching of silicon nitride". In: *Journal of Vacuum Science & Technology A* 14.4 (July 1996), pp. 2151–2157. ISSN: 0734-2101. DOI: 10.1116/1.580039. eprint: https://pubs.aip.org/avs/jva/article-pdf/14/4/2151/12007531/2151_1_online.pdf. URL: https://doi.org/10.1116/1.580039.

[22] B. E. E. Kastenmeier, P. J. Matsuo, and G. S. Oehrlein. "Highly selective etching of silicon nitride over silicon and silicon dioxide". In: *Journal of Vacuum Science & Technology A* 17.6 (Nov. 1999), pp. 3179–3184. ISSN: 0734-2101. DOI: 10.1116/1.582097. eprint: https://pubs.aip.org/avs/jva/article-pdf/17/6/3179/11018154/3179_1_online.pdf. URL: https://doi.org/10.1116/1.582097.

[23] Lee M. Loewenstein. "Selective etching of silicon nitride using remote plasmas of CF4 and SF6". In: *Journal of Vacuum Science & Technology A* 7.3 (May 1989), pp. 686–690. ISSN: 0734-2101. DOI: 10.1116/1.575866. eprint: https://pubs.aip.org/avs/jva/article-pdf/7/3/686/11447232/686_1_online.pdf. URL: https://doi.org/10.1116/1.575866.

[24] Sunghoon Lee et al. "Ultrahigh selective etching of Si3N4 films over SiO2 films for silicon nitride gate spacer etching". In: *Journal of Vacuum Science & Technology B* 28.1 (Jan. 2010), pp. 131–137. ISSN: 2166-2746. DOI: 10.1116/1.3290752. eprint: https://pubs.aip.org/avs/jvb/article-pdf/28/1/131/13926685/131_1_online.pdf. URL: https://doi.org/10.1116/1.3290752.

[25] Denise Marra and Eray Aydil. "Effect of H2 addition on surface reactions during CF4/H2 plasma etching of silicon and silicon dioxide films". In: *Journal of Vacuum Science & Technology A - J VAC SCI TECHNOL A* 15 (Sept. 1997), pp. 2508–2517. DOI: 10.1116/1.580762.

[26] R. Knizikevičius and Vitoldas Kopustinskas. "Influence of temperature on the etching rate of SiO 2 in CF 4 + O 2 plasma". In: *Microelectronic Engineering - MICROELECTRON ENG* 83 (Feb. 2006), pp. 193–196. DOI: 10.1016/j.mee.2005.08.004.

[27] URL: https://lpcvd.com/.

[28] Wikipedia contributors. *Plasma-enhanced chemical vapor deposition — Wikipedia, The Free Encyclopedia*. [Online; accessed 12-September-2023]. 2023. URL: https://en.wikipedia.org/w/index.php?title=Plasma-enhanced_chemical_vapor_deposition%5C&oldid=1167585903.